LEAD ARTICLE

Acta Cryst. (1999). B**55**, 627–663

Structural chemistry of vanadium oxides with open frameworks

Peter Y. Zavalij* and M. Stanley Whittingham

Materials Research Center and Department of Chemistry, SUNY at Binghamton, Binghamton, NY 13902-6016, USA. E-mail: zavalij@binghamton.edu

(*Received 10 August 1998; accepted 10 March 1999*)

Abstract

The present work is dedicated to a crystal-chemical and topographical analysis of vanadium oxides with open structures. The review covers, apart from a few exceptions, only pure vanadium oxide structures with vanadium in oxidation states greater than +3. Purely tetrahedral frameworks are not discussed because of their traditional, well known crystal chemistry and only a few examples of cluster compounds are provided. Structural classification and notation of vanadium oxide frameworks are proposed based on the following scheme: polyhedra → chain → layer → three-dimensional framework. Thus, approximately 60 types of vanadium oxide frameworks are divided into five classes by type of coordination polyhedra present and into 14 subclasses by a more complex structural formation. Details are also given of the analysis of vanadium–oxygen coordination polyhedra and their metamorphosis: tetrahedron–trigonal bipyramid–square pyramid–octahedron, as well as the combinatorial deduction of possible structures for the most common framework types.

Peter Y. Zavalij graduated from L'viv State University with a Masters Degree in Chemistry in 1979 and earned a Ph.D. in Inorganic Chemistry in 1984 at the same university. He started teaching as an Assistant and then Associate Professor at L'viv University. In 1993 Peter Zavalij came to the United States as a visiting scientist at the State University of New York at Binghamton and continued his research in solid-state chemistry, crystal chemistry of metal oxide intercalates and powder crystal structure determination. In 1996 he accepted a position as University Crystallographer at Binghamton University.

M. Stanley Whittingham graduated from Oxford University with a D.Phil in Chemistry studying the reactivity of the sodium tungsten bronzes. Moving to Stanford University he studied ion transport in β-alumina, for which he received the Electrochemical Society's Young Author award in 1971. His work in industry from 1972 defined the critical role of intercalation reactions in energy storage, which concept most lithium batteries use today. In 1988 he moved to SUNY as Professor of Chemistry and in 1993 was awarded a JSPS Fellowship at the University of Tokyo.

1. Introduction

There has been much interest in the last two decades in vanadium oxides and their intercalates because of their potential use as secondary cathode materials for advanced lithium batteries (Whittingham, 1976; Walk & Gore, 1975; Whittingham *et al.*, 1996) and their important role in oxidative catalysis (Vejux & Courtine, 1986). Therefore, the already rich crystal chemistry of open framework vanadates has been considerably replenished with many new structures. Such great interest in vanadium compounds is due to the variety of vanadium oxidation states and their redox properties, which readily allow the insertion or removal of ions such as lithium. The structure of these frameworks is defined in substantial part by the vanadium-oxygen coordination polyhedra, which vary from tetrahedron to trigonal pyramid, square pyramid, distorted octahedron and regular octahedron, while the oxidation state changes from +5 to +3.

Only a few structural reviews or works that include an extensive discussion of crystal chemistry have been published recently and only specific structure types are covered. Rozier *et al.* (1996) analysed the silver vanadate structures, and using structural relationships between them predicted two hypothetical structures '$Ag_xV_4O_{11}$' and '$Ag_xV_4O_{10}$'. The latter structural type was recently reported, but with tetramethylammonium instead of silver, $(tma)V_8O_{20}$ (Chirayil *et al.*, 1997). Savariault *et al.* (1996) compared sodium vanadate structures, $Na_xV_2O_5$, and Galy *et al.* (1996) discussed the network architecture of lithium vanadates with the general formula $Li_xV_{3(1+n)}O_{8+7n}$. Riou & Férey (1995) and Zhang *et al.* (1996*a*) described a structure of V_2O_5 layers built with pairs of square pyramids and tetrahedra. Zavalij *et al.* (1999) gave topographical analysis and combinatorial deduction of the simplest structures for V_6O_{14} layers constructed with zigzag chains of edge-

sharing square pyramids and tetrahedra. Galy (1992) gave a general review of vanadium oxide phases with single and double $M_xV_2O_5$ layers. Chirayil *et al.* (1998*a*) discussed hydrothermal synthetic methods for vanadium oxides in relation to their structure. The most comprehensive review of the vanadium oxide structures is provided in Wells (1986) book *Structural Inorganic Chemistry*, which describes the inorganic structures in general and, therefore, many specific details are not included. Moreover, many new structures have been published since the last edition of the book.

Therefore, a generalized review embracing the wide range of vanadium oxide structures is urgent. Even a descriptive systematization of the structure types is needed to clarify the various and very different labelings used. For example, structures with the same double-sheet octahedral layers are labeled with Greek symbols τ-$Na_xV_2O_5$, δ-$K_xV_2O_5$, ν-$K_xV_2O_5$, ε-$Ag_xV_2O_5$ and ρ-$K_xV_2O_5$ (Galy, 1992). While ρ-potassium vanadate differs from other structures in the stacking of the layers, the difference between the τ, δ, ν and ε structures is not essential and occurs mostly in the type and distribution of the intercalated ions. The lack of a comprehensive review and the existence of numerous structure types makes it almost impossible for new researchers in this field to obtain an overview in a reasonable amount of time, which sometimes leads to re-determination of structures that are claimed to be novel. Thus, the known $NH_4V_3O_8$ (Range *et al.*, 1990) was redetermined by Huang & Shan (1998).

This work presents a crystal-chemical and topographical analysis including an attempt at structural classification and a proposal for the notation of vanadium oxides with open structures. The review covers only pure vanadium oxide frameworks. Numerous structures with other transition metals and other inorganic anions, such as phosphates and sulfates, are not included in this review because in these cases the framework formation is directed very much by the peculiarities of the incorporated elements. As a further restriction, only compounds with vanadium in oxidation state greater than +3 are included, since in lower oxidation states (+3 and below) vanadium adopts regular octahedral coordination like most other transition metals. Purely tetrahedral frameworks are also not included in this review because of their traditional, well known crystal chemistry.

A structural classification of vanadium oxide frameworks is proposed and consists of two levels. First, all structures are grouped in classes by the coordination polyhedra present, then the following division into subclasses is based upon the more complex structural such as chain and layer. The suggested symbolic notation of the vanadium oxide frameworks is based on polyhedra symbols and the ways they are linked to each other, while more complex structural units such as chains, layers and three-dimensional frameworks are enclosed with different brackets. In some cases, instead of polyhedra symbols a specific symbol is assigned to particularly common chains and layers.

1.1. *Abbreviations*

Organic ligands:
tma – tetramethylammonium, $[N(CH_3)_4]^+$;
ma – methylammonium, $[CH_3NH_3]^+$;
en – ethylenediamine, $NH_2CH_2CH_2NH_2$;
enH_2 – ethylenediammonium, $[NH_3CH_2CH_2NH_3]^{2+}$;
prda – propylenediammonium, $[NH_3(CH_2)_3NH_3]^{2+}$;
ppd – piperidinium, $[NH_2(CH_2CH_2)_2NH_2]^{2+}$;
phen – phenanthroline, $C_{12}H_8N_2$;
dabco – 1,4-diazabicyclo[2.2.2]octane, $[NH(CH_2\text{-}CH_2)_3NH]^{2+}$.
Coordination polyhedra in general:
T – tetrahedron;
TB – trigonal bipyramid;
SP – square pyramid;
O – octahedron.
Coordination polyhedra in the framework:
T – tetrahedron;
U – SP with directed up apex that shares only two neighboring edges;
D – SP with directed down apex that shares only two neighboring edges;
u – SP with directed up apex that shares at least two opposite edges;
d – SP with directed down apex that shares at least two opposite edges;
O – octahedron that shares only two neighboring edges;
o – octahedron that shares at least two opposite edges;
oo – closest packed double o chain;
e – empty sites where SP or O can be expected.
Common chains and layers:
Q – quadruple O chain or layer of these chains;
X – crossed quadruple O chain;
W – wave-like O chain;
Z – UuDd chain;
ZT – UuDd chain (or layer of these chains) with two corner-sharing T.
Symbols describing frameworks:
$\langle\rangle$ – cluster or group of polyhedra;
{} – chain;
() – layer;
[] – three-dimensional framework;
$/\,/_n$ – cyclic group.
Symbols describing links:
| – edge-sharing (usually omitted);
. – sharing corner (in case of SP, corner of the base);
* – sharing apex;
.. – sharing two corners with two following polyhedra (chains);
: – sharing two corners with one polyhedron (chain);
n – used before formula to emphasize cell contents;

^{n} – (superscript) shift along the chain (y axis) relative to the previous one in terms of the polyhedra or shift with inversion if negative;

$_{n}$ – (subscript) repeat number, usually used to describe double chains or layers.

Coordinate system used for structure comparison:

x – perpendicular to the chain and parallel to the layer or to the polyhedra bases in the case of chains;

y – along the chain;

z – perpendicular to the layer or to the polyhedra bases in the case of chains.

1.2. *Symbolic structural formulae*

The general scheme for building of the structural formula is

polyhedra → chain → layer → three-dimensional framework

Thus, the following steps are used to construct the formula:

The sequence of the edge-sharing polyhedra is written using their symbols. The link symbols are also included. However, the edge-sharing symbol '|' is default and usually is omitted, since only edge-sharing is taken into account at this stage. However, in those cases where there is no edge-sharing, the sequence of the corner-sharing polyhedra may be used. Here the corner-sharing symbols '.', ':', '*' or their combination have to be included in the formula. There are possibly a few independent sequences and each of them has to be written separately.

For example, UDO or U|D|O, UUDD, uddueduude, O:T.T. *etc.*

Each sequence is put into brackets in accordance with the dimensions of the building block. Thus, angular brackets '⟨⟩' are used for clusters, braces '{}' for chains, parentheses '()' for layers and square brackets '[] ' for three-dimensional formation. However, often the high-dimensional building blocks such as layers and frameworks are conditionally subdivided into simpler blocks, usually chains, which gives a more descriptive formula.

For example, {UUDD}, (ud).

The next step is joining these formula blocks to give more complex formulation using link symbols, *e.g.* combining {UD} chains into layers ({UD}.) or {X} chains directly into three-dimensional frameworks [{X}.] or (Q) layers into frameworks [(Q).]. The dot '.' in the formula reflects the corner-sharing link of the simpler blocks into the more complex formulation. This procedure can be repeated a few times until completion. The cyclic groups of polyhedra or chains are delimited with a slash symbol '/' with a subscript index following to indicate the size of the cycle.

For example, ({UDO}.)–{UDO} chains form layers by sharing corners; {/{UD}./$_6$}–6 UD chains share corners to form a pipe; [({Q}.{UD}.).]–Q chains and UD chains share corners to form layers, which in turn also share corners to give a three-dimensional framework. The latter examples, however, may also be written as [({Q}.).{UD}.], where Q chains sharing corners form layers, which are linked into a three-dimensional framework by sharing corners with UD chains. These two formulae describe the same structure with differently chosen layers.

A bracketed delimited block may be supplied with a superscript or subscript index at the end or numerical coefficient in the front of the formula.

The superscript index is used to show the shift of the following chain or layer relative to the previous one. A negative value means a shift with inversion; *i.e.* SP with apex directed up 'u' is converted to SP with apex down 'd' *etc.*

The subscript index is used as a repeat coefficient in the following cases:

in cyclic groups, *e.g.* ⟨/u/$_8$⟩ describes a ring of eight opposite edge-sharing SPs, {/{UD}./$_6$} describes a cylinder formed with six corner-sharing UD chains;

with polyhedral symbols, *e.g.* (oooee) can be shown as (o_3e_2);

as a repeat index of a polyhedral sequence, *e.g.* {'udude'$_{-2}$} is equivalent to {ududedudue}, where a negative value has the same meaning as in the case of the superscript index;

double chain or layer, *e.g.* a quadruple Q chain can be described as two OO chains which share edges and form the more complex chain {{OO}$_2$|}.

The coefficient in front describes the number of the following blocks (usually symmetrically dependent) per unit cell, *e.g.* number of chains per repeat unit of the layer (2{UD}.) or number of layers per unit cell 2(uddue) *versus* 4(uddue). This parameter is optional and may be omitted in the general description. However, it can be used to give an idea about the total contents of the unit cell. These coefficients are used only to distinguish one framework from another or to give full structural information, which defines the unit-cell contents as well.

2. Classification of vanadium oxide structures

The richness of vanadium-oxide chemistry is due to the wide range of oxidation states and coordination polyhedra vanadium exhibits. Vanadium is often found in oxides in all the oxidation states +5, +4, +3 and even +2, whereas its neighbors in the periodic table Ti, Cr and Mn are most commonly found with the more restricted range of oxidation states: +4 and +3, +3 and +6, and +2, +4, and +7, respectively. Similarly, the typical coordination is octahedral for Ti, Cr and Mn in oxidation state +4 or less and tetrahedral for Cr and Mn in higher

oxidation states, whereas the vanadium coordination polyhedra vary from tetrahedron through trigonal bipyramid and square pyramid to distorted and regular octahedra (Fig. 1). Such a wide spectrum of coordination polyhedra gives rise to the unique and rich structural chemistry of vanadium oxide frameworks. The coordination polyhedron type correlates with the oxidation state as shown schematically in Fig. 1, where polyhedra with different coordination numbers are in different rows and those with different oxidation states in different columns. A distinguishable, but not invariable peculiarity of the V^{5+} and V^{4+} polyhedra is the presence of the vanadyl group, whose bond length (1.55–1.75 Å) is short compared with other bonds (1.9–2.0 Å for coordination numbers 5 and 6). The short bond distances in the vanadyl group, together with high VO stretching wavenumbers (940–980 cm^{-1}), provide strong evidence for VO multiple bonding (Shriver *et al.*, 1994). Very often this bond is termed double bonded and the vanadyl group is denoted as V═O, so this simplified representation will be used in this review. The *d–p* interaction of V and O involved in multiple bonding appears to be responsible for the *trans*-influence, which disfavors attachment of a ligand *trans* to the double-bonded oxygen (Shustrovitch *et al.*, 1975).

2.1. *Coordination polyhedra*

2.1.1. *Tetrahedron*. The tetrahedron (T) is a typical polyhedron for traditional *ortho*-, *meta*-, pyro-, poly- and other vanadates and in some way defines their chemical and structural similarities to phosphates. The V tetrahedron is usually more or less regular with V—O distances in the range between 1.6 and 1.8 Å, depending on the oxygen coordination. For instance, V—O distances in tetrahedral vanadium, (ma)V_3O_7 (Chen *et al.* 1999), vary from 1.61 Å for terminal oxygen, 1.71 Å for bicoordinated oxygen up to 1.79 and 1.81 Å for tricoordinated oxygen. The oxidation state of tetra-

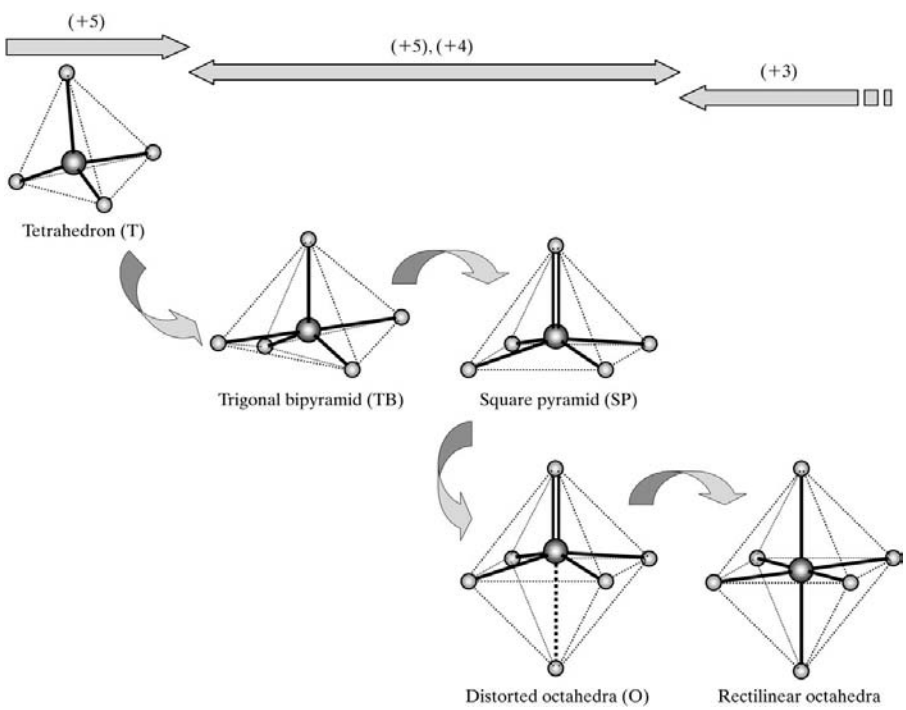

Fig. 1. Metamorphosis of the vanadium coordination polyhedra. Vertical axis: coordination number; horizontal axis: oxidation state.

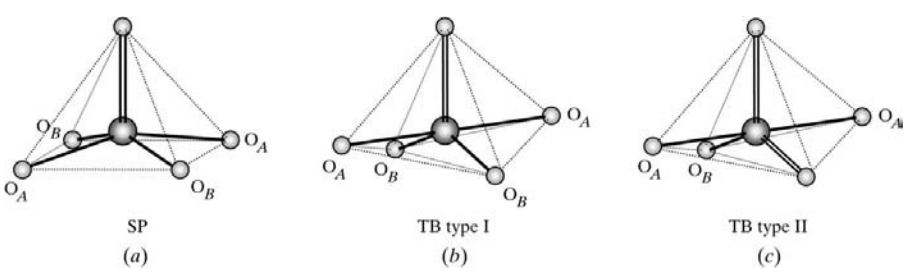

Fig. 2. (*a*) Square pyramid, (*b*) distorted trigonal bipyramid with V═O group and (*c*) distorted trigonal bipyramid with O═V═O group.

hedral vanadium is always +5 and any attempts to change it result in dramatic structural changes. Therefore, vanadium oxides with pure tetrahedral frameworks, which are usually chain-like, do not lend themselves to reversible insertion/deinsertion redox reactions and so such materials are not useful for lithium battery applications. However, their combination with other polyhedra leads to interesting layered materials.

2.1.2. *Trigonal bipyramid*. The trigonal bipyramid (TB) can be derived from T by adding a fifth O atom opposite any face and simultaneously moving the V atom to the center of this face. Typically, the TB has in its base one short V═O bond in the case of organic vanadyl complexes (type I in Fig. 2*b*) or two short bonds in the case of inorganic frameworks (type II in Fig. 2*c*). These short bonds are in the range 1.55–1.75 Å; other bonds are usually $\geq$ 1.9 Å.

2.1.3. *Square pyramid*. The square pyramid (SP) differs from TB in that four O atoms lie coplanar or almost coplanar, whereas the fifth double-bonded oxygen occupies the SP apex (Fig. 2*a*). 'Almost coplanar' cases sometimes lead to a situation when the SP is misinterpreted as a TB. The distinguishing feature of the SP is a single double-bonded oxygen in the apex at a distance of 1.55–1.75 Å from V, and more or less four coplanar O atoms in the base at distances of 1.9–2.1 Å. In contrast, the TB (type II) generally has in its base two double-bonded oxygens at shorter V—O distances and the third at 1.8–1.9 Å.

To distinguish between SP and TB (type I) quantitatively, the angular structural parameter τ was proposed by Addison *et al.* (1984). The τ parameter is defined as: $\tau = (\beta - \alpha)/60$, where α and β are O_A—V—O_A and O_B—V—O_B, respectively (Fig. 2*a*), assuming that $\beta \geq \alpha$. For purely SP polyhedra τ is 0 and for a perfect TB polyhedron τ is 1. Corman *et al.* (1997) applied this parameter and described vanadyl complexes with $0 < \tau \leq 0.5$ as distorted SP, while complexes with $0.5 < \tau < 1$ were considered as distorted TB. Thus, two out of five new molecular vanadyl complexes were described as having SP and three as having TB coordination. This ratio, however, is not common and could be induced by the chelating ligand, substituted salicylaldehyde. In contrast to this work, Allen & Kennard (1993) analysed 56 five-coordinated monomeric vanadium complexes with a single vanadyl group and found only one compound, VO(quinolinol)$_2$ (Shiro & Fernando, 1971), contained a distorted TB (τ = 0.56). It will be shown in this work that inorganic frameworks also have five-coordinated vanadium in SP only, except some cases of mixed-metal frameworks. It is difficult to apply the τ criterion to TB with two short V═O bonds (Fig. 2*c*) simply because the apex may be chosen in two different ways and very often both choices are almost identical in geometry. It is very clear, even without applying the τ criterion, that five-coordinated vanadium with two double oxygens has TB polyhedra: three O atoms of the base make O—V—O angles close to 120°, whereas two apical atoms have this angle close to 180°.

In this work the following subdivision of the five-coordinated polyhedron was used:

In the presence of one V═O bond the τ criterion is applied to distinguish SP and TB.

Coordination polyhedra with two V═O bonds are considered as distorted TB.

Thus, there are three types of five-coordinated polyhedra in vanadium oxide structures. The metamorphosis of the tetrahedron to trigonal bipyramid and square pyramid is illustrated in Fig. 3. Two VO_3 chains of corner-sharing tetrahedra interact with each other by forming an additional fifth V—O bond, shown as a dashed line in Fig. 3 to form a V_2O_6 double chain while keeping the same two terminal O atoms double bonded. Therefore, the V coordination is predetermined as TB type II (Fig. 2*c*). However, generating the V_2O_5 layer from a series of double chains by sharing corners leaves only one terminal O atom and that defines SP coordination.

2.1.4. *Distorted octahedron*. Adding one more O atom on the base converts the SP into a distorted octahedron (O), as shown in Fig. 1. The peculiar feature of this polyhedron is that the short V═O bond remains almost without changes and the additional oxygen moves into a position opposite and forms a weak V···O bond, whose length is 2.1 Å or more. Another problem, how to distinguish between distorted O and SP, arises here: how weak can the new bond be or, in geometrical terms, how far can the additional oxygen be from V and still be considered as bonded? For example, the well known α-modification of V_2O_5 (Enjalbert & Galy, 1986) is built from SP layers, but the V coordination polyhedra can include an oxygen from the next layer, giving distorted octahedral coordination. A statistical and geometrical analysis of the structures, presented in this work, shows that most often the V···O distance lies between 2.2 and 2.35 Å, however, it can vary from 2.1 Å up to 2.6 Å. The last value was considered as the upper limit for a weak V···O bond based on the statistical distribution of V—O bond lengths and topographical analysis. In the case of V_2O_5 the additional sixth O atom is at 2.79 Å from V and, therefore, should not be included in coordination

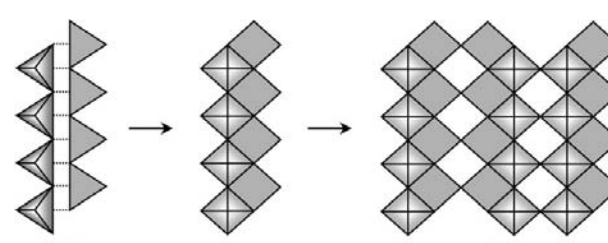

Fig. 3. Transformation of two T chains through a TB double chain into an SP layer.

using the 2.6 Å limit. Nevertheless, very often the limit of 3 Å is used and then V_2O_5 is described as layers of octahedra that share corners and in such a way form a three-dimensional framework. It was found that the distorted octahedron can be derived not only from SP, but also from the distorted TB (type I in Fig. 2) by adding an extra oxygen opposite the V═O bond, which remains short in the octahedron as well. This type of distortion can be distinguished from the SP distortion by applying the same SP–TB criterion. Another type of octahedron distortion can be derived from the tetrahedron by adding two O atoms on the two faces opposite the short V═O bonds. The length of the V═O bonds remains unchanged or changes only slightly up to 1.8 Å, two other bonds from tetrahedra retain their length in the 1.8–1.9 Å range and two newly formed bonds opposite the V═O groups are weak with lengths 2.1 Å and more. This type of distortion can be derived from TB type II also, but distortion of the tetrahedron is simpler and more obvious. These three ways of octahedron distortion can be described as square-pyramidal, trigonal-pyramidal and tetrahedral.

2.1.5. *Regular octahedron*. The three previous polyhedra, TB, SP and O, are typical for vanadium with oxidation states from +5 to +4. Moving to the lower oxidation states of +3 and below changes the coordination polyhedra to a regular octahedron, the traditional octahedron typical of 3*d* transition metals in low oxidation states. The short V═O bonds with lengths 1.6–1.7 Å and weak V···O bonds with lengths usually much over 2.1 Å disappear when a distorted octahedron converts to the regular octahedron or in other words all V—O bonds become equal or almost equal with lengths 1.9–2.1 Å.

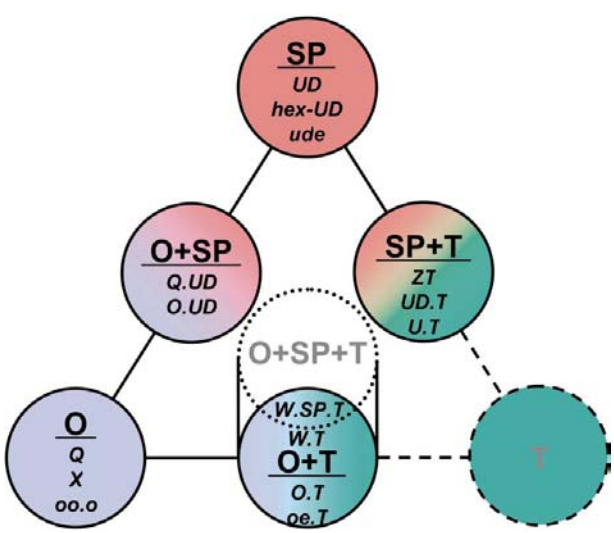

Fig. 4. Classification of the vanadium oxide frameworks. Structural classes and subclasses are shown in bold and italic, respectively.

The metamorphic changes of coordination polyhedra from tetrahedron through trigonal bipyramid and square pyramid to distorted and then regular octahedron in the oxidation state range from +5 to +3 are schematically shown in Fig. 1. At least part of this chain TB–SP–distorted O–regular O, which permits a wide range of oxidation states, is promising for intercalation/deintercalation chemistry and, therefore, for applications such as cathode materials for secondary lithium batteries. The work performed by Bergström *et al.* (1997) has shown how distorted octahedra change into regular octahedra during lithium intercalation into a V_6O_{13} framework. Such continuous changes in coordination polyhedra in parallel with changes in the oxidation state allow the insertion of a relatively large amount of lithium and its extraction without breaking the structure apart, an essential requirement for the multiple charge/discharge process in rechargeable batteries.

2.2. *Classification by coordination polyhedra and structural units*

The structures of vanadium oxide frameworks can be thought of as composed of polyhedra that link to form chains, which in turn link into layers and then three-dimensional frameworks

polyhedron → chain → layer → three-dimensional framework.

Obviously, only a few structures can be completely decomposed in this way. The two middle links of the scheme, chain and layer are treated as building blocks. In this work, chains are defined as composed of edge-sharing polyhedra, while layers are composed of corner-sharing chains. However, in some cases it is convenient to define chains that only share corners or layers where all polyhedra share only corners or only edges. In these cases it is always pointed out each time when the chain or layer is used in a definition different from that given above.

A class of vanadium oxide is defined and named by the coordination polyhedra which form the framework; *e.g.* the SP class includes all vanadium oxide structures built from square pyramids, and the O + T class is built from both octahedra and tetrahedra. As shown schematically in Fig. 4, only six classes can be deducted from three types of polyhedra: T, SP and O. The colors in Fig. 4 are used throughout this review to distinguish between the SP (pink), O (violet) and T (green) polyhedra. Notice that some polyhedra and classes are not found in the scheme:

The TB are not included, because they exist only in such compounds as monomeric metal-organic compounds and clusters, mixed-metal frameworks, and vanadate chains, which are outside the scope of this review.

The regular and distorted octahedra are not separated in the scheme. One of the reasons is that they can be converted into each other simply by changing the oxidation state without significant changes in the V—O framework.

The tetrahedral class (T) is shown only for completeness of the scheme, but its structural characteristics are not discussed in this review since T represents traditional valence compounds with a fixed oxidation state +5.

The most complex combination of O, SP and T has a single representative, but this is more conveniently treated as a member of the O + T class.

By this system all vanadium oxide frameworks are divided into five classes: SP, SP + T, O, O + SP and O + T. Each class is subdivided, usually by the type of chain or the ways in which the polyhedra link together, in two to four subclasses giving 14 subclasses in total. In turn each subclass joins up to seven structure types or around 60 types all together. The five classes of the vanadium oxide frameworks are discussed in the following chapters, which start with the description of chains and finish with examples of clusters.

3. SP and O chains

This chapter covers the chains of square pyramids and octahedra as building blocks for vanadium oxide frameworks. Some chains exist in real structures as separate units, but in others they are linked into layers or frameworks.

3.1. *SP chains*

The three configurations of chains formed from square-pyramidal polyhedra are presented in Fig. 5. The first type (Figs. 5*a–c*) is built by SP sharing neighboring edges of the base. When this type of sharing occurs, the SP is marked with capital letter 'U' and 'D' for apex directed up and down, respectively, and therefore this type is termed a UD chain. The second type of SP chains, shown in Figs. 5(*d*) and 5(*e*), reflects another way of SP joining, when opposite edges of the base are shared. In this case the lower case 'u' and 'd' are used and the chains are termed ud chains. The third type of SP chain, shown in Fig. 5(*f*), combines both types of sharing, when some polyhedra share neighboring edges and some opposite edges. This type is termed a UuDd chain. Thus, the sequence of four letters U, D, u and d can describe any of the SP chains, and '{}' are used as separators to identify the chain in more complex formations.

3.1.1. *UD chains*. The first chain (*a*) in this series is the simplest and its symbol is {U} or {UU} if the repeat unit has to be represented. However, this chain does not exist separately, but was found as a building block in V_3O_7 (Waltersson *et al.*, 1974). The {UU} chain can also be used to describe more complex chains. Alternating U and D polyhedra form the next {UD} chain (*b*). This well known chain exists by itself in VO_3^- polyvanadates

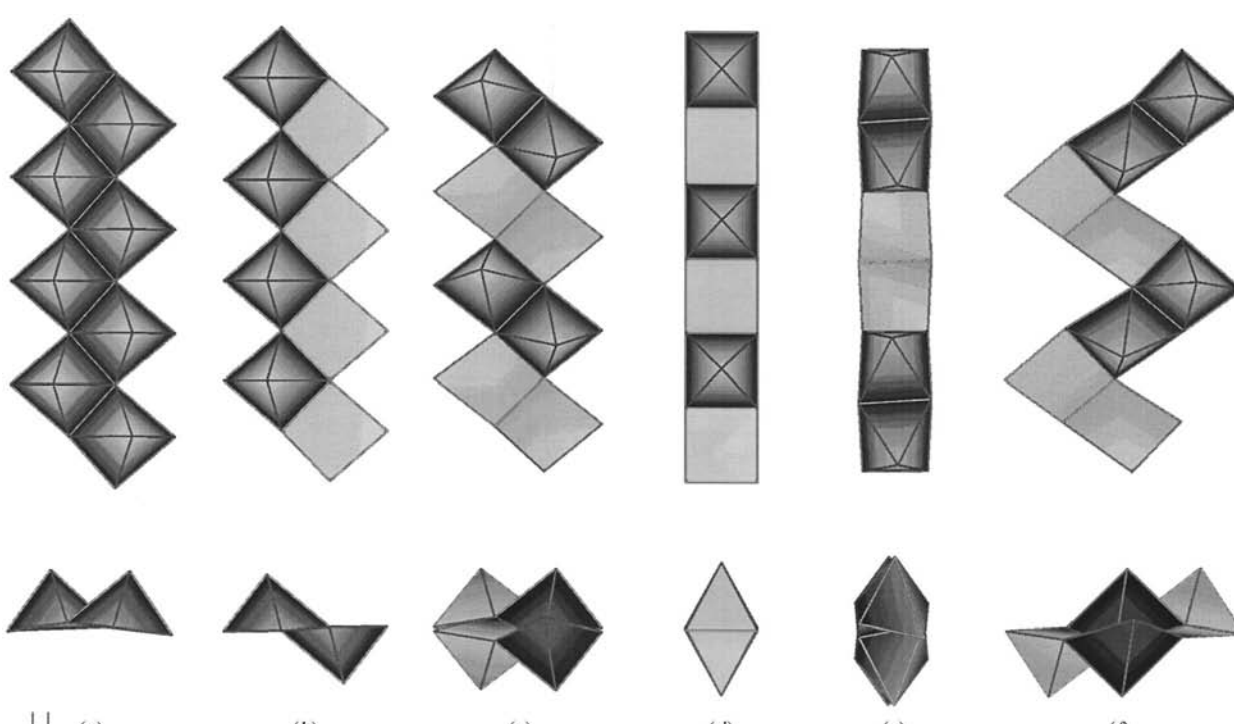

Fig. 5. SP chains: (*a*) {UU}, (*b*) {UD}, (*c*) {UUDD}, (*d*) {ud}, (*e*) {uudd} and (*f*) {UuDd} = {Z}.

Table 1. *SP chains*

Compounds shown only when an individual chain exists.

Fig. 5	Chain symbol	Repeat distance (Å)	Compound	Reference
(*a*)	{UU}	3.65		
(*b*)	{UD}	3.65	$NaVO_3$	(1)
			$NaVO_3.1.9H_2O$	(2)
			$KVO_3.H_2O$	(3)
			$Ca(VO_3)_2.4H_2O$	(4)
(*c*)	{UUDD}	6.9 (7.3)†	$Co(VO_3)_2.4H_2O$	(5)
(*d*)	{ud}	5.2		
(*e*)	{uudd}	9.9 (10.4)	$VO(OCH_2CH_2O)$	(6)
(*f*)	{UuDd} ≡ {Z}	6.5–6.7 (7.3)†		

† Idealized value. (1) Kato & Takayama (1984); (2) Bjoernberg & Hedman (1977); (3) Evans (1960); (4) Ahmed & Barnes (1963); (5) Avtamonova *et al.* (1990); (6) Weeks *et al.* (1999).

(Table 1), often with trigonal bipyramidal distortion (type II), and is found as a building block of UD layers in such well known compounds as V_2O_5, NaV_2O_5, δ- and γ-LiV_2O_5 *etc.* (see §4.1 and 4.2). The last in the UD series is {UUDD}, where a down-directed pair follows an up-directed SP pair. This chain is found by itself in $Co(VO_3)_2.4H_2O$ (Avtamonova *et al.*, 1990) and as a building block within a layer in $(tma)V_4O_{10}$ (Zavalij *et al.*, 1996; see §4.1).

The ud chains (Figs. 5*d* and 5*e*) consist of opposite edge-sharing SPs. They share edges to form ud layers (see §4.3). Some SPs in these chains can be vacant and these are marked as empty with the symbol 'e'. So, in addition to {ud}, the following chains {udue}, {udude} and {uddue} can be extracted as building blocks from the ud layers. Nevertheless, the {uudd} chain exists separately in the structure of vanadyl glycolate (Weeks *et al.* 1999; Fig. 6).

So far, the UuDd series with both types of edge-sharing has only one representative – the {UuDd} chain that was discovered recently in $V_6O_{14}^{2-}$ layers (see §5.1). The SPs sharing the neighboring and the opposite edges alternate when the SPs are directed up and down in pairs. This defines a zigzag configuration of the chain (Fig. 5*f*), which in further discussion is labeled as a {Z} chain.

The repeat distances along the chain are shown in the third column of Table 1. For the UD and UuDd chains the diagonal of the SP base goes along the chains, whereas for the ud series the chains are parallel to the edge of the SP base. The average lengths of the diagonal and the edge are 3.65 and 2.6 Å, respectively. Thus, the repeat distance along the chain is proportional to these values, but only in the {UD} and {ud} cases, whereas {UUDD}, {uudd} and {UuDd} chains are much shorter than expected, *e.g.* 6.6 Å *versus* 7.3 Å (2 × 3.65) in {UUDD}. The reason for this shrinkage of these chains is the alternation of two SPs up and two SPs down, whereas in the previous case single SPs alternate. The two pyramids have apexes going in the same direction and are, therefore, substantially tilted, as shown in Fig. 6, which causes shortening of the chain. According to this scheme the tilt in the {UU} and hypothetical {u} chains should lead to the formation of rings, as found in the clusters $V_{12}O_{32}$, $V_{18}O_{42}$, $V_{15}O_{36}$ and $V_{22}O_{54}$ (see §9).

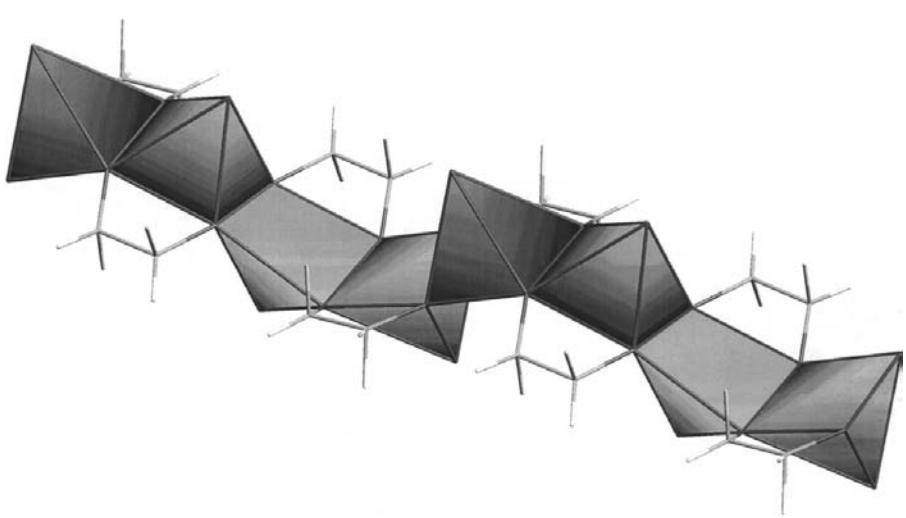

Fig. 6. Individual {uudd} chain in the $VO(OCH_2CH_2O)$ structure.

Table 2. *Symmetry groups for UD chains*

No.	Anti-symmetry of the symbol at the UD pair $\bar{1}$	Symmetry of the symbol at: U or D m_Y	Symmetry of the symbol at: UU or DD 2_Z	Translation symmetry $\Sigma = 2n+1$ b_X	Translation anti-symmetry $\Sigma = 4m+2$ 2_1	Translation anti-symmetry $\Sigma = 4m$ b_Z	Simplest symbol (the part generated by translation anti-symmetry is underscored)	Rod group
1	Yes	Yes	(No)	(No)	(Yes)	(No)	**UD**	$\wp 2_1/m$
2		No	Yes	(No)	(No)	(Yes)	**U$\underline{\mathbf{UDD}}$**	$\wp 112/b$
3			No	(No)	(No)	(No)	UU$\underline{\mathrm{DD}}$UD	$\wp\bar{1}$
4	No	Yes	Yes	(Yes)	(No)	(No)	$(\mathbf{U})_2$	$\wp bm2$
5			No	(No)	(No)	(No)	UUUD	$\wp m$
6		No	Yes	(No)	(No)	(No)	UUUUDD	$\wp 2$
7			No	Yes	(No)	(No)	$(\mathrm{UUUDDUD})_2$	$\wp b11$
8				No	Yes	(No)	UUUUDUU$\underline{\mathrm{DDDDUDD}}$	$\wp 2_1$
9					No	Yes	UUUDUU$\underline{\mathrm{DDDUDD}}$	$\wp 11b$
10						No	UUUUDDUD	$\wp 1$

3.1.2. *Symmetry deduction*. The chain symbols can be used not only to describe the frameworks, but also to deduce the symmetry for all possible chain configurations, as shown in Table 2. This deduction is based on the fact that the symmetry of the symbol corresponds with the geometric symmetry of the chain. Two types of symbol symmetry are possible: reflection and translation.

The reflection means that the symbol can be divided into two parts related to each other as mirror images. The division of the symbol by single U or D letters (column 3 in Table 2) corresponds to a geometric mirror plane (m_Y), which is perpendicular to the chain (y axis). The division by UU or DD pairs (column 4 in Table 2) causes a twofold rotation axis (2_Z) perpendicular to the chain and to the SP base (z axis).

The translation means that the symbol consists of finite repeat units corresponding to the repeat unit of the chain. The repeat unit of the symbol should only contain even numbers of letters to be coincident with the geometric repeat unit. If it does not, the symbolic repeat unit has to be doubled and an additional geometric symmetry element appears (column 5 in Table 2), which is glide plane (b_X) parallel to the chain and perpendicular to the SP base with translation along the chain. For example, in UDUDU both U and D divide the infinite symbol into symmetric parts and the repeat unit is UD, whereas in UUU both the single U and UU pair are dividers and the repeat unit UU is doubled.

Antisymmetry of the symbol is based on the definition that U is asymmetric to D, which indicates antisymmetry in the SP orientation. It is obvious that the symbol can be divided (reflected) into antisymmetric parts only by the UD pair (column 2 in Table 2), which corresponds to the geometric inversion center in the middle of this pair. The antisymmetric translation means the presence of two repeat units inverted to each other and alternating along the chain symbol. This antisymmetry of the symbol corresponds to a twofold screw axis along the chain (column 6 in Table 2), when the number of letters in the antisymmetric unit is odd; otherwise, the glide plane parallel to the SP base with translation along the chain (column 7 in Table 2) results. For example (line 2 in Table 2), in $\cdots$UUDDUU$\cdots$ UD pairs divide the symbol into antisymmetric parts UU and DD, which can also be converted into each other with antisymmetric translation UU into DD and *vice versa*.

This leads to the ten symmetry groups of UD chains. Three of them, $\wp 2_1/m$, $\wp 2/b$ and $\wp bm2$, represent known chains. These are the simplest cases (two or four polyhedra per repeat unit) with the highest symmetry.

Table 2 can also be applied to mixed chains with symbols containing u and d letters in addition to U and D. In that case the caption of the third and fourth columns should be expanded with 'uu, dd, u or d' and the Σ in the following columns means the sum of U and D symbols only. Thus, the only known {UuDd} chain possesses the eighth row in the table with $\wp 2_1$ symmetry.

The purely ud chains are quite different and were analysed separately in a similar way, as shown in Table 3. The second and third columns describe the antisymmetric and symmetric division (reflection) of the symbol with single letters or pairs, whereas the fourth column is related to the antisymmetric translation. The presence of unoccupied positions in the ud layers or letters 'e' in the symbol has no effect on this deduction, except it has to be mentioned that 'e' is antisymmetric to itself and, therefore, it can divide the symbol into both symmetric and antisymmetric parts. Thus, there are only five symmetry types of the ud chains, but all known chains, including those from ud layers, belong to the first case with the highest symmetry *pmmb*. Again, because of the tilt (puckering) between two similarly oriented SPs, the simplest chain {u} was not found, except as the circle formation in the clusters (see §9).

Table 3. *Symmetry groups for ud chains*

	Antisymmetry	Symmetry	Translation antisymmetry		
No.	2_X	m_Y	b_Z	Simplest symbol	Rod group
1	Yes	Yes	(Yes)	**ud**	$\wp mmb$
2		No	(No)	uduudd	$\wp 2/m11$
3	No	Yes	(No)	u	$\wp mm2$
4		No	Yes	uddu<u>uduuddd</u>	$\wp m2_1b$
5			No	uduuddd	$\wp m11$

3.2. *O chains*

Chains of edge-sharing octahedra are shown in Fig. 7. Two of them (Figs. 7*a* and 7*d*) might be considered as parental for the two groups of O chains. In the first {OO} chain the octahedra share two perpendicular edges with a common corner, whereas in the second {o} chain the opposite edges are shared. Notice that two 'O' symbols in the first case and only one 'o' in the second case are used to reflect the repeat unit of the chain.

Two {OO} double chains superimposed along the *z* axis form quadruple chains. In one case (Fig. 7*b*), the {OO} chains are shifted half a diagonal of the octahedra base along the chains (*y* axis), in another case (Fig. 7*c*), the chains are shifted perpendicularly to the chain along a direction which defines the *x* axis for this type of chain. In order to simplify symbolic formulae, these two new formations are designated as {X} and {Q} chains, respectively. The relation of these chains to the SP chains (in this case {UU}) and the arrangement of weak V···O bonds is shown in Figs. 8(*a*) and 8(*b*), where only the half of the octahedron that contains the double-bonded oxygen in the apex is colored. The other half is transparent, so the week V···O bond can be viewed. However, Fig. 8(*c*) shows a different circular distribution of the weak V···O bonds. These variations of the {Q} chains are defined by how the chains are linked to each other.

The second group of O chains, where opposite edges are shared, starts from the simplest {o} chain (Fig. 7*d*). This chain has the ability to build double and triple chains and even layers by sharing two edges from each octahedron. The specific feature of these multiple formations is the closest packing of the O atoms where metal atoms occupy octahedral cavities. However, only single {o} and double {oo} chains are found in the vanadium oxide structures discussed here. The double {oo} chain is shown in Fig. 7(*e*) and can be used to derive unusual wave-like chains (Fig. 7*f*) by removing each third octahedron. From another point of view, this type of chain (marked {W}) is a single chain of octahedra with semiadjacent sharing edges.

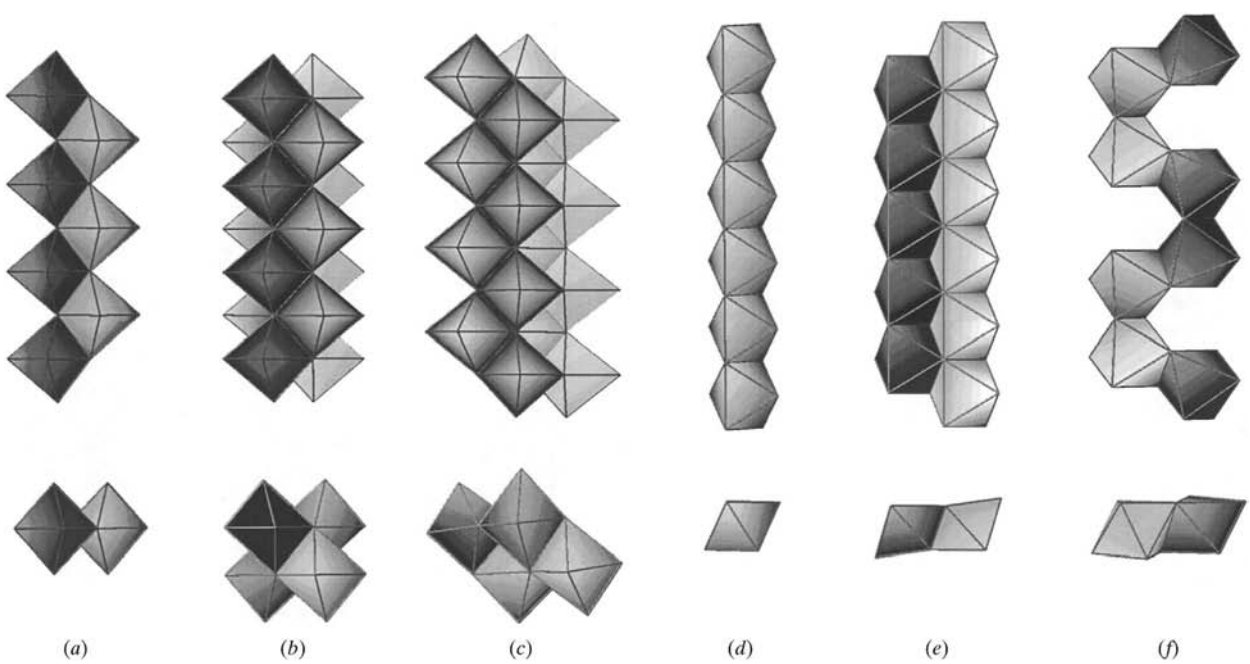

Fig. 7. O chains: (*a*) double chain {OO}, (*b*) crossed quadruple chain {X}, (*c*) quadruple chain {Q}, (*d*) opposite edge-sharing chain {o}, (*e*) double o-chain {oo} and (*f*) wave-like chain {W}.

Table 4. *Deduction of UD and UUDD layers*

Transormation represents the symmetry operation that transforms one chain into the adjacent chain. The symbol of the second chain starts at the same level as for the first chain.

Chain symbol	Rod group	Transformation	Layer group	Symbol	Fig. 10
{UD}	$\wp 2_1/m$	m_x	*pmmn*	(2{UD}.)	(*a*)
		'2*y*'	'*c*2/*m*'	({UD}.{DU}.)	(*b*)
{UUDD}	$\wp 112/b$	m_x	*pmab*	(2{UUDD}.)	(*c*)
		2*y*	*pbab*	({UUDD}.{DDUU}.)	Hypothetical
		2*z*	*p*112/*b*	({UUDD}.{DUUD}.)	
		$\bar{1}$	*p*112/*b*	({UUDD}.{UDDU}.)	

The only O chains that were found as separate units are the {Q} chain in M_xVO_3 compounds (see §6.1) and the {o} chain in $Ba_2V_3O_9$ (Dhaussy *et al.*, 1996; Mueller-Buschbaum & Feldmann, 1996; Fig. 9*a*). The latter is actually surrounded by corner-sharing tetrahedra. A chain of corner-sharing octahedra was found in vanadyl acetate (Weeks *et al.*, 1999; Fig. 9*b*) and also as a structural unit in the three-dimensional framework of V_3O_7 (Waltersson *et al.*, 1974). However, this chain is not common.

4. SP structures

This section covers the open framework vanadium oxide structure with only square pyramidal coordination of vanadium. This type of structure forms the SP class, which can be divided into three subclasses:

layered UD structures built from corner-sharing UD chains;

UD pipes also built from corner-sharing UD chains that form hexagonal tunnels;

layered ud structures, whose layers are constructed directly from SPs sharing three or four edges with each other.

4.1. *UD structures*

As already mentioned in §3.1, UD chains are formed with SPs that share two neighboring edges. Only three of ten possible UD chains are found among known structures: {UU}, {UD} and {UUDD} (Table 2). They can be linked into layers differently depending on how the apices of corner-sharing SPs from adjacent chains are directed (Fig. 10).

The first chain, {UD}, forms two different layers with equally and oppositely directed apexes of corner-sharing SPs from adjacent chains, while the second more complex type of chain, {UUDD}, can form four different layers, as shown in Table 4. Both types of UD layer (2{UD}.) (Fig. 10*a*) and ({UD}.{DU}.) (Fig. 10*b*) have real representatives (Table 5), whereas, only one of the four possible UUDD layers is known in its single representative $(tma)V_4O_{10}$, discovered recently by Zavalij *et al.* (1996).

The simplest UD layer (2{UD}.) is one of the most common (therefore, most studied) vanadium oxide structures, including the parental vanadium pentaoxide V_2O_5. The stacking of the layers can be different: one or two layers per unit cell. Obviously, in the first case layers are simply translated along the *z* axis, so that the apex of each SP is opposite the V═O group of the SP from another layer. In the second case every other layer is shifted along the chains (*y* axis) for a half SP. To distinguish between these cases the number of layers per unit cell can be added in the front of the layer symbol,

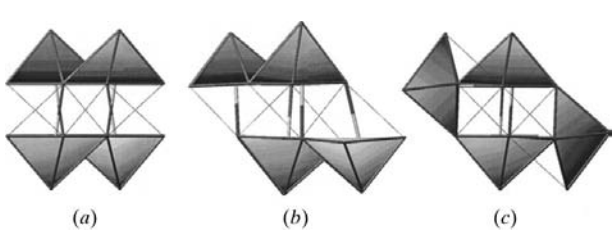

Fig. 8. Distribution of weak V···O bonds in the quadruple octahedral chains: (*a*) {X} chain; (*b*) {Q} chain – parallel distribution; (*c*) {Q} chain – circular distribution.

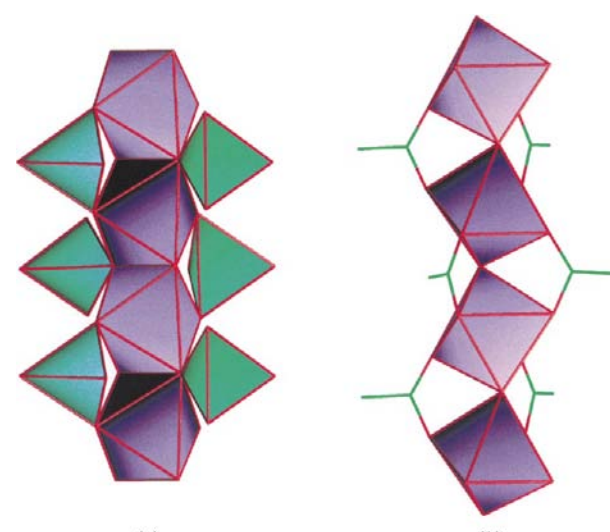

Fig. 9. (*a*) Chain of edge-sharing octahedra {o} in $Ba_3V_3O_9$ and (*b*) chain of corner-sharing octahedra {O.} in $VO(CH_3COO)$.

Table 5. *UD layers*

The space group in the coordinate system is used in this work (see §2.1).

Fig. 10	Formula	Compound	Space group	*a* (Å)	*b* (Å)	*c* (Å)	Reference
(*a*)	(2{UD}.)	α-V_2O_5	*Pmmn*	11.51	3.56	4.37	(1), (2)
		α-$Li_xV_2O_5$, $x = 0.04$	*Pmmn*	11.46	3.55	4.37	(3)
		$x = 0.10$		11.50	3.57	4.39	(4)
		ε-$Li_xV_2O_5$, $x = 0.45$	$P2_1mn$	11.41	3.56	4.52	(4)
		$x = 1.00$		11.36	3.59	4.68	(5)
		α'-NaV_2O_4F	*Pmmn*	11.32	3.61	4.80	6
		α'-NaV_2O_5	$P2_1mn$	11.32	3.61	4.80	7
		CaV_2O_5	*Pmmn*	11.35	3.61	4.89	8
		$Cu_{0.64}V_2O_5$	*Pmmn*	11.31	3.61	4.80	9
	2(2{UD}.)	δ-LiV_2O_5	*Amma*	11.24	3.60	9.91	(10)
				11.25	3.70	9.92	(11)
		MgV_2O_5	*Amma*	11.02	3.69	9.97	(11), (12)
(*b*)	2({UD}.{DU}.)	γ-LiV_2O_5	*Pnma*	9.70	3.61	10.66	(13)
		γ-V_2O_5	*Pnma*	9.95	3.59	10.04	(14)
(*c*)	2({UUDD}..)	$(tma)V_4O_{10}$	$B2_1ma$	11.74	6.64	17.12	(15)

(1) Enjalbert & Galy (1986); (2) Bachmann *et al.* (1961); (3) Hardy *et al.* (1964); (4) Dickens *et al.* (1979); (5) Murphy *et al.* (1979); (6) Carpy & Galy (1971); (7) Carpy & Galy (1975); (8) Bouloux & Galy (1976); (9) Christian & Mueller-Buschbaum (1974); (10) Cava *et al.* (1986); (11) Millet *et al.* (1998); (12) Bouloux *et al.* (1976); (13) Galy *et al.* (1971); (14) Cocciantelli *et al.* (1991); (15) Zavalij *et al.* (1996).

e.g. 2(2{UD}.) in δ-LiV_2O_5 and MgV_2O_5. In the case of one layer stacking, the inter-layer interaction is due to very weak V···O bonds with length 2.79 Å in V_2O_5 between the V atom from one layer and the terminal (double-bonded) O atom from the next layer. Another peculiarity of the single layer unit cell is the interlayer distance, which as shown in Table 5 varies from 4.37 to 4.89 Å depending on the amount and type of ions intercalated between the layers. Intercalation of a small amount of metal species, *e.g.* $x = 0.04$–0.10 in $Li_xV_2O_5$ practically does not change the interlayer distance from pure V_2O_5. Increasing the amount of metal ions between the layers causes a jump in the interlayer spacing by as much as 0.4–0.5 Å. The weak V···O bonds break (the V···O distance extends to 3.29 Å in NaV_2O_5), but the layer structure is probably stabilized by extra electron density in place of weakly bonded oxygen, while layers are held together by electrostatic forces. This is similar to the two layers stacking 2(2{UD}.) in δ-LiV_2O_5 and MgV_2O_5, where a weak V···O bond is not formed due to the shift of every other UD layer.

In contrast to (2{UD}.), where two chains are transformed to each other by reflection, two chains in the second type of UD layer, ({UD}.{DU}.), are transformed to each other by a ~120° rotation around shared corners (*y* axis), thereby resulting in two symmetrically independent chains. These chains form layers, when the rotation angle alternates in sign (Fig. 10*b*, bottom).

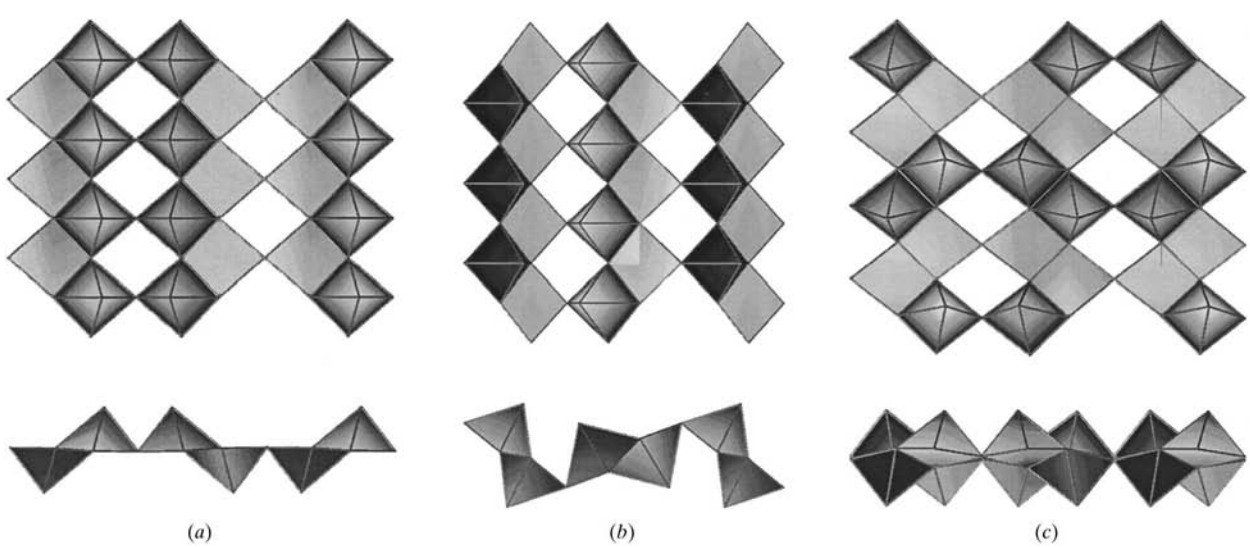

Fig. 10. Layers from SP chains: (*a*) ({UD}.), (*b*) ({UD}.{DU}.) and (*c*) ({UUDD}.).

Table 6. *UD pipes*

Fig. 11	Formula	Compound	Space group	a (Å)	c (Å)	Reference
(*a*)	{/{UD}./$_6$}	$Cs_{0.3}V_2O_5$	$P6_3/m$	14.36	3.61	Waltersson & Forslund (1977*a*)
(*b*)	[{/{UD}./$_6$}.3{UD}.]	$Cs_{0.35}V_3O_7$	$P6_3/m$	9.88	3.61	

Otherwise, when the angle does not alternate, the layer bends into a pipe, as found in the hexagonal UD structures described in the following section (Fig. 11). The specific feature of this type of layer, which distinguishes it from a simple (2{UD}.) layer, is the different distribution of weak V···O bonds. Thus, in γ-V_2O_5 these bonds are 2.71 Å between the layers and 3.11 Å within the layers between two corner-sharing chains, whereas in the simple V_2O_5 all the weak bonds are 2.791 Å in length and occur between the layers only. Intercalation of Li increases the interlayer spacing and, therefore, makes these bonds almost equal in length (3.07 and 3.17 Å in γ-LiV_2O_5).

As can be seen from Fig. 10(*c*), the chains in UUDD layers are significantly buckled due to the presence of two equally directed SPs in pairs. As already mentioned in §3.1, this buckling is obvious since two neighboring SPs with the same orientation tend to put their apexes apart. This is why the repeat unit along the chain in $(tma)V_4O_{10}$ is 6.64 or 2×3.32 Å, which is substantially shorter than expected from the simple {UD} chain value of 7.4 (2×3.7) Å.

The stoichiometry of the UD layers is always V_2O_5 since they are constructed from V_2O_6 UD chains sharing two corners. Therefore, to describe all structures constructed of the UD chains the general formula V_nO_{2n+1} can be used, where n is the number of chains sharing corners and is 1 for the chain and 2 for the layer structures.

4.2. *UD pipes*

These frameworks built from hexagonal pipes (Fig. 11) look unusual. Nevertheless, they are constructed as described in the previous section. {UD} chains share SP corners in such a way that they can be transformed to each other by a 120° rotation, which is always in the same sense in contrast to ({UD}.{DU}.) layers where the sense of rotation alternates. The rotation angles in the layered structures are ± 116 and ± 122° for γ-LiV_2O_5 and γ-V_2O_5, respectively.

Two types of UD pipes are known and each is represented by a single caesium vanadate (Table 6). The first structure, $Cs_{0.3}V_2O_5$, consists of hexagonal pipes (Fig. 11*a*), which are built from six UD chains sharing corners in a circle. Cs atoms fill the space inside and between the pipes. The second structure is a three-dimensional framework built from the same hexagonal pipes (Fig. 11*b*), which share faces with each other. This structure is more difficult to describe with the proposed symbolic formula. Thus, the formula given in Table 6 consists of two parts: the first, /{UD}./$_6$, describes the hexagonal pipes and the second depicts {UD} chains as links between these pipes. However, these two parts of

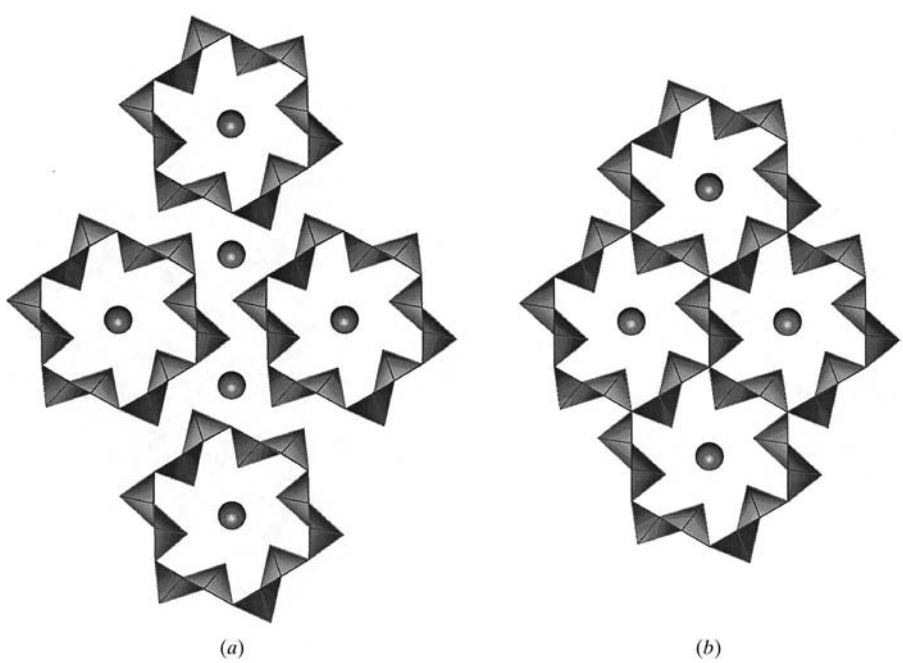

Fig. 11. Hexagonal tunnel structures from UD chains: (*a*) one-dimensional hexagonal pipe, /{UD}./$_6$ and (*b*) three-dimensional framework of hexagonal pipes [/{UD}../$_6$].

Table 7. *ud layers*

Fig. 12	Formula	Compound	$a_1 \times a_2$	$b_1 \times b_2$	a_{clc} (Å)	b_{clc} (Å)	SP/cell	Defect	Space group	a (Å)	b (Å)	c (Å) γ (°)	Reference
(*a*)	2{ud^{1}|}	$Li_xV_{2-\delta}O_{4-\delta}$	1 × 1	−1 × 1	3.70	3.70	2	~1/6	*P*4/*nmm*	3.69		6.79	(1)
		$Li_xV_{2-\delta}O_{4-\delta}.H_2O$							*I*4/*mmm*	3.71		15.80	(2)
(*b*)	2{2{udue}$^{-1}$|}	CaV_3O_7	4 × 0	0 × 2	10.47	5.23	8	1/4	*Pnam*†	10.46	5.30	10.38	(3)
(*c*)	({ududedude}^{7}|)	CaV_4O_9	3 × 1	−1 × 3	8.27	8.27	10	1/5	*P*4/*n*	8.33		5.01	(4)
(*d*)	2{{uddue}^{3}|)	α-$Cs_2V_4O_9$	2 × 1	−1 × 2	5.85	5.85	5	1/5	$P4_2/m$	5.73		15.05	(5)
		$Rb_2V_4O_9$							$P4_2/m$	5.68		14.74	(5)
	4{{uddue}^{3}|)	β-$Cs_2V_4O_9$							$I\bar{4}2d$	5.73		30.06	(5)
(*e*)	2{{uddueduude}^{8}|)	(ppd)V_4O_9	4 × 2	−1 × 2	11.70	5.85	10	1/5	$P112_1/a$†	11.72	5.86	16.85	(6)
												91.2	

† Converted to the setting used in this work. (1) Chirayil *et al.* (1996*a*); (2) Chirayil *et al.* (1996*b*); (3) Bouloux & Galy (1973*a*); (4) Bouloux & Galy (1973*b*); (5) Liu & Greedan (1995); (6) Zhang *et al.* (1998).

the formula describe the same objects of the structure. The alternative symbol [..{UD}..] does not represent hexagonal pipes as structural units, but it depicts the fact that each side of the UD chain shares corners with two other chains. From this point of view, this is a unique case where three UD chains share their corners. In contrast to the previous structure, in $Cs_{0.35}V_3O_7$ only the channels are filled with Cs atoms.

The $Cs_{0.3}V_2O5$ structure is very similar to γ-V_2O_5 (Table 5) in weak V···O contacts present: 2.87 Å in length between and 3.17 Å within (between two corner-sharing chains) the pipes for the first structure *versus* 2.71 Å between and 3.11 Å within the ({UD}.{DU}.) layers in γ-V_2O_5. In contrast to the previous structure, in the $Cs_{0.35}V_3O_7$ structure only one type of weak V···O bond with length 3.12 Å exists, those between corner-sharing chains. The hexagonal $Cs_{0.35}V_3O_7$ structure can be shown as a combination of already known ({UD}.{DU}.) layers from γ-V_2O_5 (Table 5) linked into a three-dimensional framework by corner-sharing {UD} chains, *i.e.* [({UD}.{DU}.).{UD}.].

The stoichiometry of the UD pipes can be described as V_nO_{2n+1}, which is essentially the same formula used for UD layers and UD chains, where n also has the same meaning (number of chains sharing corners), which is 2 for $Cs_{0.3}V_2O_5$ and 3 for $Cs_{0.35}V_3O_7$.

4.3. *ud structures*

This type of layer is built from SPs in the same way as the UD layers. However, it differs in the way SPs are linked together. In the case of UD layers the polyhedra share two edges to form chains, which in turn form layers sharing corners, whereas in the case of ud layers all polyhedra can share two, three or four edges, forming layers in which no corner-sharing chains can be defined. So far the five types of ud layers shown in Fig. 12 have been found. The SPs alternate in orientation often in a chessboard order. Some of the SPs are vacant.

The symbolic formulae of these layers (Table 7) are generated in the same way as before: first the chain of SPs is written as a sequence of lower case symbols 'u' and 'd' (since each SP shares opposite edges) and 'e', which represent an empty site. The multiplier before the chain is used to define the unit-cell content, while the following superscript shows the number of SP adjacent chains shifted relative to each other. These chains form ude layers by sharing edges, which is indicated by the vertical line '|' following the chain symbol. The optional multiplier in front of the delimiting layer parenthesis defines the number of layers per unit cell. This gives a full description of the layer, nevertheless, the short formulae, which include the ude sequence delimited by parentheses only, can be used as well.

The base edges of the SP are used to define a coordinate system to describe the unit cell of the ude layer. Thus, the columns '$a_1 \times a_2$' and '$b_1 \times b_2$' in Table 7

contain **a** and **b** of the two-dimensional unit cell expressed as vectors in the SP basis. The next two columns give **a** and **b** values in Å, calculated assuming 2.62 Å as the average length of the SP base. The column 'SP/cell' gives the number of SPs including empty sites per two-dimensional unit cell and is equal to $[(a_1^2 + a_2^2)(b_1^2 + b_2^2)]^{1/2}.\sin\gamma$, where γ is the angle between **a** and **b** that differs from 90° in the distorted lattice.

The simplest, parental (ud) layer shown in Fig. 12(*a*) was discovered recently by Chirayil *et al.* (1996*a*,*b*) in lithium vanadates (Table 7). It is a layer of SPs alternating up and down in strict chessboard order. Therefore, each polyhedron shares four edges with neighboring SPs with an opposite orientation. However, about 1/6th of the V sites are vacant in a disordered manner in these two structures. Both the hydrated and dehydrated compounds contain the same vanadium oxide layer, but with a different stacking; in the hydrated compound the terminal O atoms in two adjacent layers are directed to each other to form a short O···O contact of 3.11 Å in length. Whereas in the absence of water, the layers are simply translated along **z** so the SP apex from one layer is opposite the SP base from another. The Li atoms were not localized, but they occupy a supposedly vacant SP site and/or a similar position on the other side of the base of the SP opposite the V atom. The same ud layers are found in the $MgVO_3$ structure (Bouloux *et al.*, 1976). However, in this case the layers share corners forming a three-dimensional framework $[(ud)^*]$, which is possible because alternating chains of SPs are occupied by Mg atoms rather than V atoms. Therefore, this structure could be used as indirect proof of a possible occupation disorder of V and Li atoms in $Li_xV_{2-\delta}O_{4-\delta}$, since Mg is the crystal-chemical analog of Li. However, the lithium ions can be removed electrochemically, leading to a new form of VO_2 (Chirayil *et al.*, 1996*b*). This suggests Li in an interlayer site rather than in the vacant SP site.

The next two structures in Table 7, CaV_3O_7 and CaV_4O_9 (Figs. 12*b* and 12*c*), are directly derived from the parental (ud) with an ordered distribution of the empty sites, which occupy 1/4 and 1/5 of all sites, respectively. The orientation of the SPs in the remaining sites is in the strict chessboard order. Thus, replacing the 'e' symbols in their 'udue' and 'udude' formulae with 'd' and 'u', respectively, will lead to the parental structure (ud).

However, the last two structures of this series (Figs. 12*d* and 12*e*) have a different distribution of the SP orientations that cannot be reduced to the (ud) layer. An interesting feature of all V_4O_9 layers (*c*–*e*) is the presence of only two sequences, 'udude' and 'uddue', or

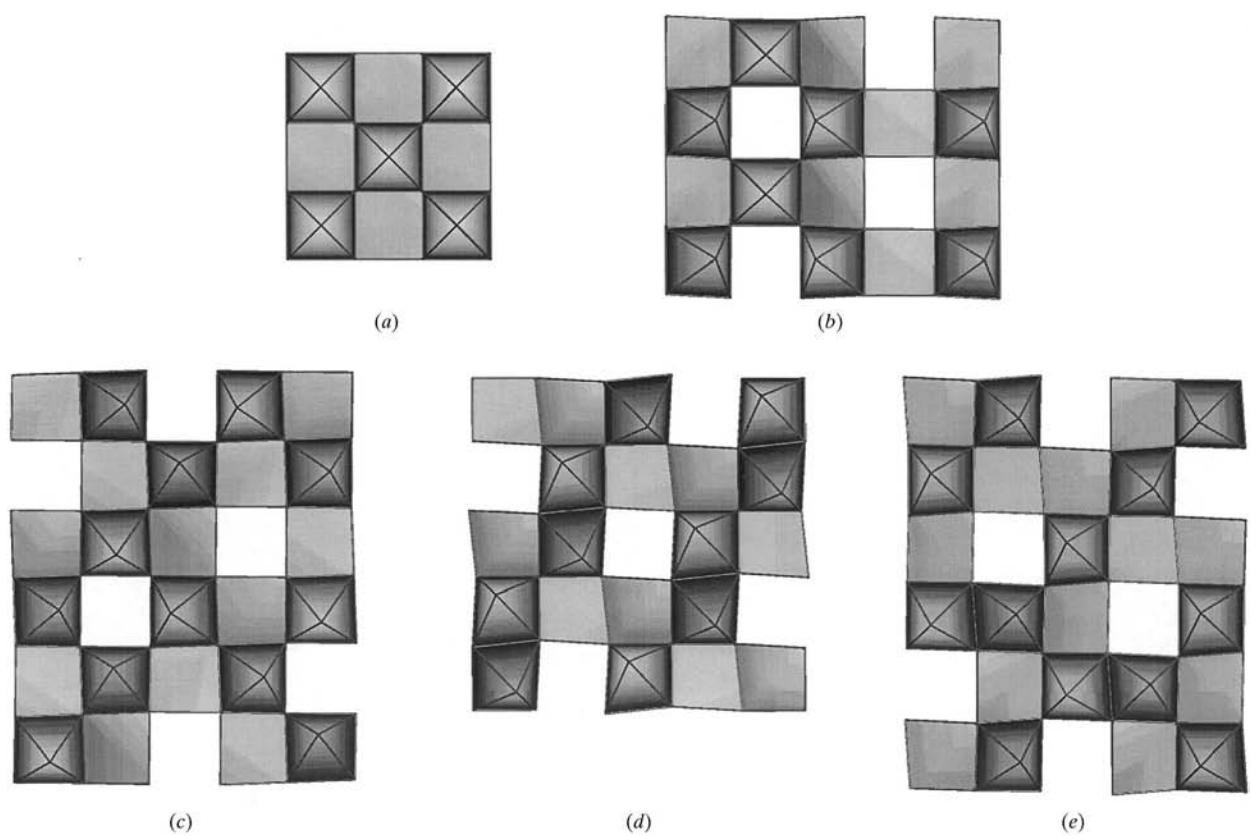

Fig. 12. Chess-like (ude) layers: (*a*) $(ud)^1$, (*b*) $(udue)^{-1}$, (*c*) $(ududedudue)^7$, (*d*) $(uddue)^3$ and (*e*) $(uddueduude)^8$.

their inverted images and this formula sequence might be different for vertical and horizontal directions. For example, CaV_4O_9 (*c*) has the same sequence in both directions 'udude' or, for completeness, 'ududedudue', whereas in $Cs_2V_4O_9$ and $Rb_2V_4O_9$ (*d*) the sequences in perpendicular directions are antisymmetric 'uddue' and 'duude'. The third case, $(ppd)V_4O_9$ (*e*), has completely different sequences 'uddue' in the horizontal chains and 'udude' in the vertical chains, having an intermediate configuration between (*c*) and (*d*) layers. Another property of the three layers with 1/5 empty sites is that all the SPs share three edges, while it is four in the case of the simple (ud) layer and mixed two and three in the case of the (udue) layer. The UD layers can also be described in these terms as layers with 1/3 unoccupied sites, where each SP shares only two edges with others.

The topographical derivation of the layers with 1/5 empty sites (1/5 layers) was conducted using two rules: three-edge sharing by each SP and prohibition on placing two empty sites next to each other. The empty sites taken as a starting point were built up step by step with occupied SPs obeying the rules. At some point, as shown in Fig. 13, the decision has to be made which of the sites introduced next are to be empty. Only two choices appear, which are shown in the figures by solid and dashed circles. However, they are equivalent under a 90° rotation. Therefore, it can be assumed that applying the 'three-edge sharing with no neighboring empty sites' rules leads only to the distribution of the 1/5 empty sites shown in Figs. 13(*c*)–(*e*). These differ only in their SP orientations. In spite of the difference between these three structures, they are built from identical blocks – four SPs sharing edges and alternating up and down forming in this way 2 × 2 squares. The squares share edges with four others and form layers that differ only in the relative orientation of the squares distinguished by the letters A and B in Fig. 13. Another possible configuration of the 2 × 2 square is labeled C in Fig. 13. However, the C square cannot exist because the apices of two equally directed SPs have to be tilted, but the UU and DD pairs have to be tilted in opposite directions. The latter defines the third rule: equally directed SPs sharing edges are not allowed in the 2 × 2 square. Another configuration of the square UDDD cannot exist because of the same reason.

Finally, using A and B squares just three simple layers can be built, as shown in Fig. 13: [A] B4 where each square shares edges with four others in the opposite orientation, [A] A4 where all squares are identically oriented, and [A] ABAB where two squares are in the same orientation as the original square and two are opposite. Only these three layers have been found (Figs. 12*c*–*e*). It can be shown that the [A]AABB and [A]ABBB configurations lead to lower symmetry and more complex layers and, therefore, to more complex symbolic sequences. For example, the first configuration

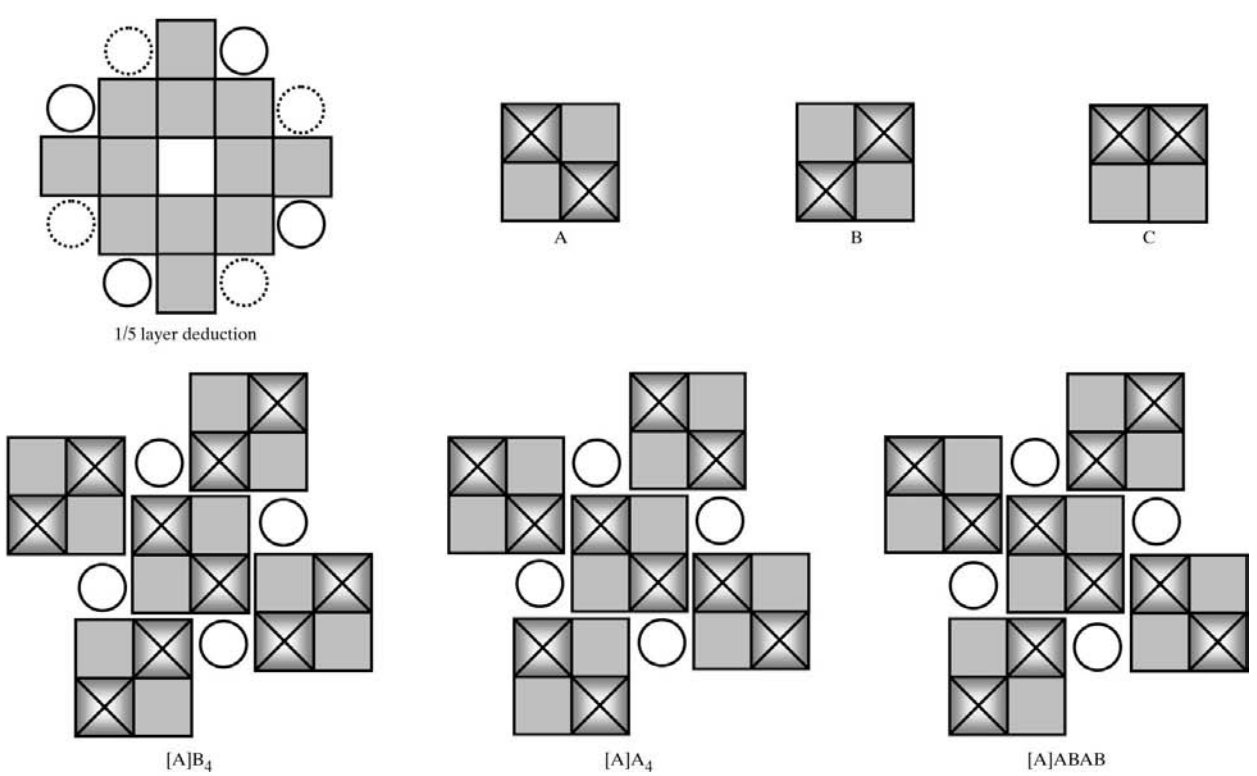

Fig. 13. 1/5 'ud' layers and their building blocks.

Table 8. *U-T layers*

Fig. 14	Formula	Compound		Space group	*a* (Å)	*c* (Å)	Reference
(*a*)	(/U./$_3$.2T.)	$K_3V_5O_{14}$	$K_3(VO_2)_3(VO_4)_2$	*P*31*m*	8.69	5.01	(1)
(*b*)	2(U./T./$_4$.)	$Cs_2V_5O_{13}$	$Cs_2VO(VO_3)_4$	*I*4*mm*	7.76	11.75	(2)
(*c*)	(U.⟨T.T⟩.)	$Rb_2V_3O_8$	$Rb_2VO(V_2O7)$	*P*4*bm*	8.92	5.55	(3)
		$K_2V_3O_8$	$K_2VO(V_2O_7)$	*P*4*bm*	8.87	5.22	(4)
		$(NH_4)_2V_3O_8$	$(NH_4)_2VO(V_2O_7)$	*P*4*bm*	8.89	5.56	(5)
		$(H_3O)_2V_3O_8$	$(H_3O)_2VO(V_2O_7)$	*P*4*bm*	8.91	5.58	(6)

(1) Evans & Brusewitz (1994); (2) Waltersson & Forslund (1977*b*); (3) Ha-Eierdanz & Mueller (1992); (4) Galy & Carpy (1975); (5) Range & Zintl (1988); (6) Hagrman *et al.* (1998).

gives the 'uddueduedue' sequence, where both the single SPs and the SP pairs alternate. Supposedly it can be realized in the presence of a few intercalated ions to induce complexity in the layer. This restriction can be formulated as the fourth rule: the sequences of occupied SPs, which lie between empty sites along one direction, have to be symmetrically dependent – equal or anti-symmetrically equal to each other.

As can be seen from Table 7 the calculated and observed intralayer cell parameters match very well, except the (uddue) layer – the case where 'uu' or 'dd' pairs are present in the chains in both directions. Owing to the tilt between the pair of equally directed SPs the cell dimensions for CaV_4O_9 (32° tilt) are contracted by ~3%. However, this contraction is much less than, for example, ~5% in an individual {uudd} chain of $VO(OCH_2CH_2O)$ with a 43° tilt, probably owing to the higher flexibility of a one-dimensional chain *versus* a two-dimensional layered formation. The tilt in the uu pair for $(ppd)V_4O_9$ is 20°, which is substantially less.

In spite of its complex appearance, the 'ud' symbolic formula is more informative and can be used to describe other types of layers as well. Thus, the UD layers (Table 5) can be represented as chains of opposite edge-sharing SPs with 1/3 vacant sites. Thus, (2{UD}.) in V_2O_5 can be described as ($\{udedue\}^1$) with unit-cell vectors 3×3 and -1×1; the ({UD}.{DU}.) layer in LiV_2O_5 can be described as ($2\{ude\}^1$) with the same vectors, and the (2{UUDD}.) layer in $(tma)V_4O_{10}$ as ($\{uueduedeude\}^7$) with vectors 3×3 and -2×2.

The general stoichiometry of the ud layers is V_nO_{2n+m} and reflects the ratio between occupied (n) and vacant (m) SPs. Thus, $n = 1$ and $m = 0$ for the parental VO_2 layer, whereas for other known layers m is always 1 while n is 3 and 4, giving V_3O_7 and V_4O_9 compositions for the layers. Notice, that since UD layers can be represented as ud layers with 1/3 vacant sites, the V_2O_5 stoichiometry also results from the ud layers' general formula V_nO_{2n+1} for $n = 2$, but with a different definition of the coefficient n.

5. SP-T structures

This type of vanadium oxide structure is built from two types of coordination polyhedron: square pyramids and tetrahedra. The division of SP-T structures into subclasses was based on joining the SPs in more complex formations that leads to three types of structures:

In the first type, U-T, the SPs are separate units and are joined by sharing corners.

In the second type, UD-T, two, three or more alternating SPs share edges to form UD blocks, which are linked into the layer by sharing corners with tetrahedra and other blocks.

In the last type, the Z-T structures, {UuDd} zigzag chains labeled as {Z} chains are linked into layers by sharing corners with tetrahedra.

5.1. *U-T structures*

These layered structures are composed of corner-sharing square pyramids and tetrahedra. All SPs share four corners with either tetrahedra or other SPs. Similarly, all tetrahedra share three corners. In both cases one corner remains terminal. All this defines $V_{n+m}O_{3n+5m/2}$ stoichiometry, where n and m are the number of SP and T, respectively. The specific feature of these layers is that all terminal O atoms are located on one side of the layer. Therefore, only the U symbol is used for square pyramids. This configuration of the layers along with their equal orientation means that no inversion center, any horizontal axis or any plane can be present, leading to uncommon space-group symmetry (Table 8).

The first type of U-T layer (Fig. 14*a*) is built from blocks of three SPs corner linked to form a triangle. Formed in this way /U./$_3$ cycles are linked into the layer by sharing the remaining corners of the base with isolated tetrahedra. A 3:2 SP/T ratio gives V_5O_{14} layer stoichiometry.

The second U-T type (Fig. 14*b*) consists of a cyclic tetramer of corner-sharing tetrahedra V_4O_{12} or $(VO_3)_4$ – well known formations in tetravanadates and phosphates. These tetramers share corners with isolated SPs to form layers. Here a 1:4 ST/T ratio yields a V_5O_{13} layer.

The third structure (Fig. 14*c*) represented by three compounds is built in a similar way to the latter, except that a simple dimer V_2O_7 or pyrovanadate group is used instead of a tetramer. To emphasize the structure the two columns with chemical structural formula are given

Table 9. *UD-T layers*

Fig. 15	Formula	Compound	Space group	*a* (Å) *α* (°)	*b* (Å) *β* (°)	*c* (Å) *γ* (°)	Reference
(*a*)	(UD.2T..)*α*	CsV_2O_5	$P2_1/c$	7.02	9.90 90.7	7.78	(1)
(*b*)	(UD.2T..)*α′*	$Ca(V_2O_5)_2.5H_2O$	$P\bar{1}$	6.36 110.2	18.09 101.6	6.28 82.9	(2)
		$enH_2(V_2O_5)_2$ (1*a*)	$P\bar{1}$	6.60 109.6	7.64 104.8	5.98 82.3	(3)
		$enH_2(V_2O_5)_2$ (1*b*)	$P\bar{1}$	6.25 78.7	6.40 80.2	7.47 77.2	(3), (4)
		$(prda)(V_2O_5)_2$	$P2_1/n$	8.00	10.01	15.70	(5)
		$(ppd)(V_2O_5)_2$	$P\bar{1}$	6.39 94.5	6.42 105.9	8.20 104.0	(4)
(*c*)	(UD.2T..)*β*	$(ppd)(V_2O_5)_2$	$P2_1/n$	9.36	6.43 105.8	10.39	(3)
(*d*)	({{⟨UUD⟩.}$_2$:⟨T.T⟩}..2T.)	$(en_2Cu)_2(V_2O_5)_5$	$P\bar{1}$	8.91	15.93	6.73	(6)
(*e*)	({U⟨UD⟩$_4$D.T.UDD.T.UD.T.}.)	$(tma)_5(V_2O_5)_9$	$P\bar{1}$	12.66 78.7	15.36 74.4	16.96 83.3	(7)

(1) Waltersson & Forslund (1977*c*); (2) Konnert & Evans (1987); (3) Zhang *et al.* (1996*a*); (4) Riou & Férey (1996); (5) Riou & Férey (1995); (6) Zhang, DeBord *et al.* (1996); (7) Koene *et al.* (1998).

in Table 8: gross formula and formula with tetrahedral groups shown separately in parentheses, where VO_4 is orthovanadate, V_2O_7 is di- or pyrovanadate, and $(VO_3)_4$ denotes cyclic tetravanadate. Therefore, such compounds are often termed vanadyl vanadates, *e.g.* vanadyl tetravanadate (*b*) or vanadyl divanadate (*c*). The SP/T ratio of 1:2 generates a V_3O_8 stoichiometry for this layer.

5.2. *UD-T structures*

This type of layer also consists of SP blocks and T sharing corners. The SP blocks are found to be simple pairs of edge-sharing SPs with opposite orientations ⟨UD⟩, ⟨UUD⟩ trimers where the middle SP shares two adjacent edges, and more complex ⟨UUDUDUDUDD⟩ decamers where the middle section of eight SPs is a part of the {UD} chains common for layered SP structures. Since T always shares three corners and SP blocks share all terminal and bicoordinated O atoms of the SP base the UD-T structures have V_2O_5 stoichiometry with a constant O:V ratio.

The pairs of SPs ⟨UD⟩ linked into the layer by sharing corners with separate tetrahedra form a group of structures with the general symbol (UD.2T..) (Table 9). The layer content V_2O_5 can be also represented as $VO(VO_4)$ to reflect the presence of the vanadyl group (V^{4+}) and the orthovanadate group (V^{5+}) in the struc-

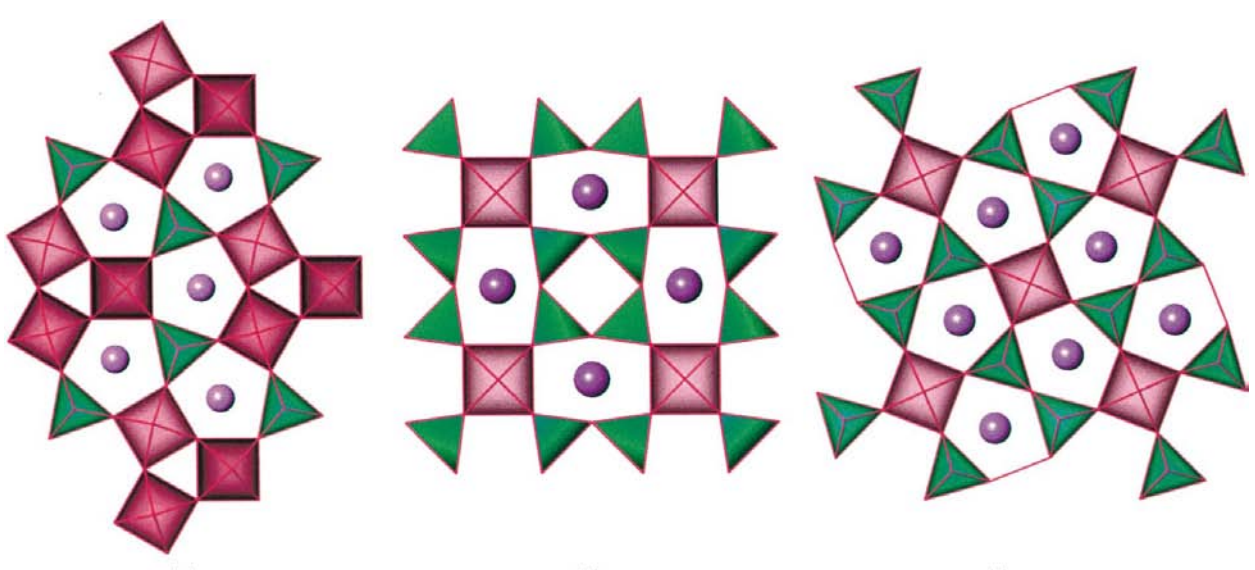

Fig. 14. Layers built up from separate SP and T: (*a*) (/U./$_3$.2T.), (*b*) (U./T./$_4$.) and (*c*) (U.⟨T.T⟩.).

ture. Three different ways to connect ⟨UD⟩ with T are realized in structures shown in Figs. 15(*a*)–(*c*), which are labeled with α, α' and β, respectively.

The first two layers α and α' are essentially the same, except for the orientation of the tetrahedra. All ⟨UD⟩ groups in α and α' layers are parallel to each other with rows of tetrahedra between them (Figs. 15*a* and 15*b*). In the α layer the orientation of the tetrahedral apex (terminal oxygen) alternates from row to row, whereas in the α' layer the alternation is along the row. However, in the β layer the ⟨UD⟩ pairs form rows in which the pair is rotated by 90° around the axis perpendicular to the layer (Fig. 15*c*). The β structure has another distinguishable difference – the bases of all the polyhedra are practically coplanar, while in the α and α' layers they are noticeably tilted. Each T shares three corners with two SPs directed up and two down (one corner is double shared) and, therefore, the orientation of T up or down does not seem very important. Nevertheless, the α layer is found only in CsV_2O_5, but the α' layer has five known representatives (Table 9) and also is found in vanadyl phosphates, *e.g.* $VO(HPO_4).1/2H_2O$ (Leonowicz *et al.*, 1985). This is probably due to the intercalated ions present. Thus, the α structure is formed with unhydrated metal ions, whereas hydrated metal ions and organic cations prefer the α' structure.

The next $(V_{10}O_{25})^{4-}$ layer has the complex structure (Fig. 15*d*). ⟨UUD⟩ and ⟨DDU⟩ trimers of edge-sharing SPs share corners to form the {⟨UUD⟩.} chain. Half the tetrahedra, coupled into V_2O_7 divanadate groups, sharing two corners from each tetrahedron link two chains into a flat double chain $\{\{\langle UUD\rangle.\}_2{:}\langle T.T\rangle\}$. The other half, single tetrahedra of VO_4 vanadate groups, join the double chains into step-like layers.

The last structure, $(tma)_5V_{18}O_{45}$ or $(tma)_5(V_2O_5)_9$ (Fig. 15*e*), is complex, however, it can be described by ⟨UD⟩ dimers, ⟨UUD⟩ trimers and long ⟨UUDUDUDUDD⟩ groups that share corners and form a {⟨UUDUDUDUDD⟩.⟨UDD⟩.⟨UD⟩.} chain. Tetrahedra sharing two corners additionally link these groups within the chain. Finally, these chains form layers by sharing corners, some parts of which resemble ({UD}.) layers. Moreover, these chains can be converted to UD chains by transforming the tetrahedra to square pyra-

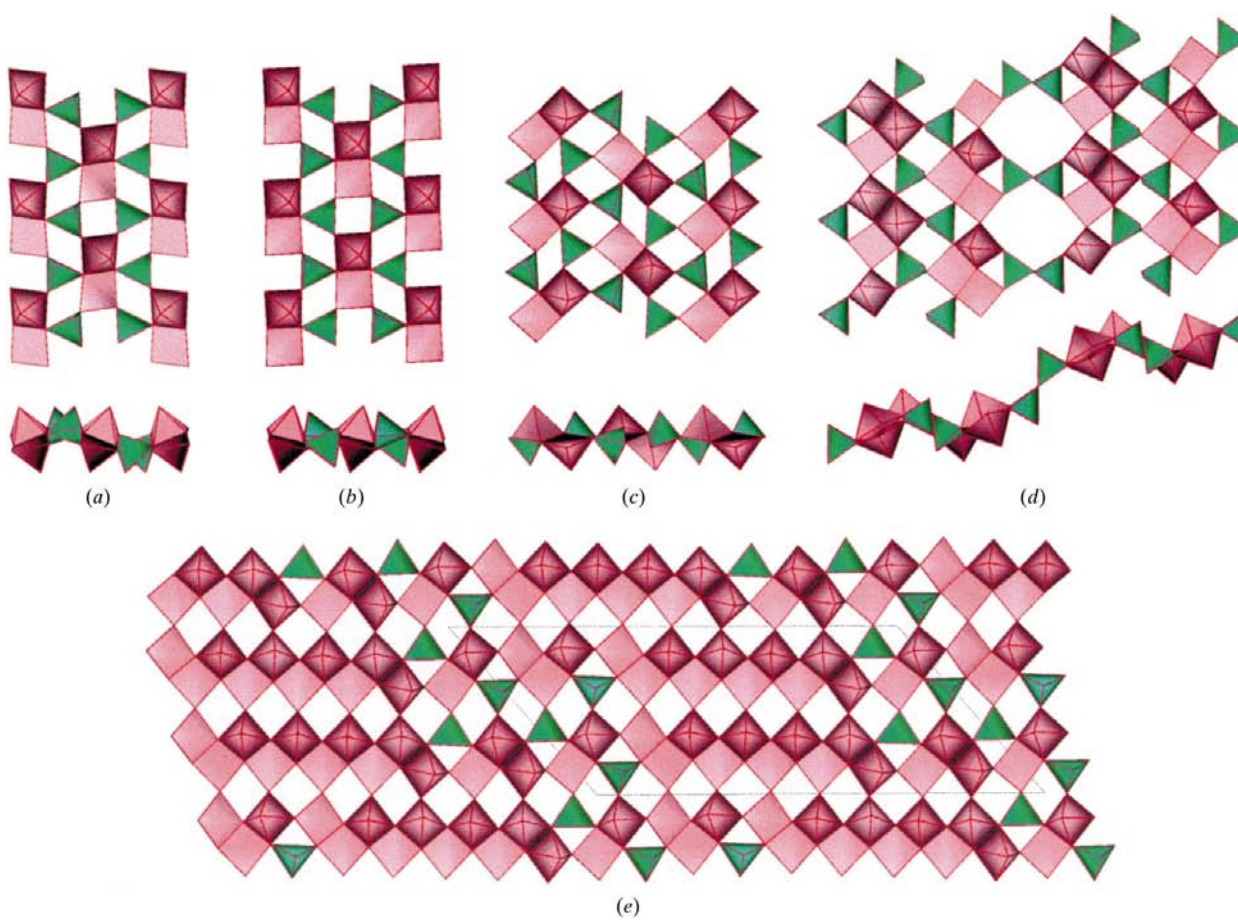

Fig. 15. Layers built up from UD blocks and T: (*a*) α-(UD.2T..), (*b*) β-(UD.2T..), (*c*) γ-(UD.2T..), (*d*) ($\{\{\langle UUD\rangle.\}_2{:}\langle T.T\rangle\}$..2T.) and (*e*) ($\{U\langle UD\rangle_4D.T.UDD.T.UD.T.\}$.).

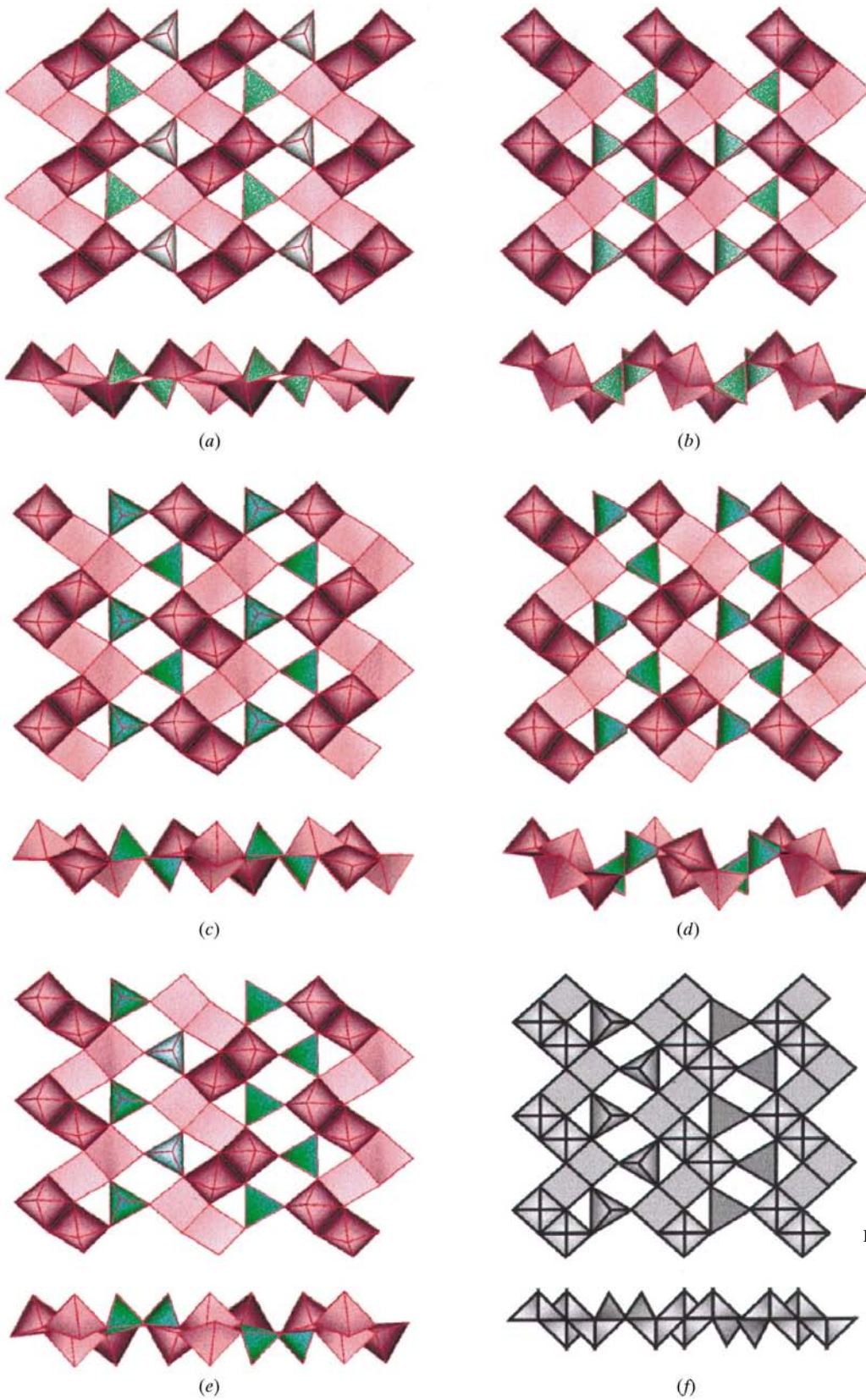

Fig. 16. Z-T layers ({UuDd}:2T.): (*a*) α in (*tma*)V_3O_7, (*b*) α' in (*dabco*)$V_6O_{14}.H_2O$, (*c*) β in (en_2M)V_6O_{14} (M = Zn, Cu), (*d*) β' in (*ma*)V_3O_7, (*e*) γ in (en_2Ni)V_6O_{14} and (*f*) δ, hypothetical.

Table 10. *Z-T layers*

Space group in the coordinate system is used in this work.

Fig. 16	Formula	Compound	Layer symmetry	Space group	a (Å)	b (Å)	$1/c^*$(Å)	Reference
(*a*)	({UuDd}:T.)α	(tma)V_3O_7	$p2_1$	$P2_1/n$	8.43	6.55	2 × 9.24	(1)
(*b*)	({UuDd}:T*)α'	(dabco)$V_6O_{14}.H_2O$	$p2_1$	$A2$	7.55	6.63	2 × 8.95	(2)
					7.57	6.66	2 × 8.99	(3)
(*c*)	({UuDd}:T.)β	$(en)_2ZnV_6O_{14}$	$p2_1/a$	$P2_1/a$	2 × 8.37	6.53	8.33	(4)
		$(en)_2CuV_6O_{14}$	$p2_1/a$	$P2_1/a$	2 × 8.33	6.56	8.29	
(*d*)	({UuDd}:T*)β'	(ma)V_3O_7	$p2_1/a$	$P2_1/a$	2 × 7.60	6.66	7.90	(5)
(*e*)	({UuDd}:T.)γ	$(en)_2NiV_6O_{14}$	$pb2_1a$†	$P112_1/a$	2 × 8.30	6.63	2 × 8.56	(6)
(*f*)	({UuDd}:T.)δ	Hypothetical	$p2_12_12$					

† The layer in the title structure is deformed ($\alpha = 90.17^\circ$) and therefore its symmetry is $p11a$. (1) Zavalij *et al.* (1997*a*); (2) Nazar *et al.* (1996); (3) Zhang *et al.* (1996*b*); (4) Zhang, DeBord *et al.* (1996); (5) Chen *et al.* (1999); (6) Zavalij *et al.* (1999).

mids. This requires only a ∼0.3 Å shift for V and two O atoms of T groups to the middle of the chain. This derived chain would be {UUDUDU-DUDDUUDDUUDD} or {⟨DU⟩$_3$⟨DDUU⟩$_3$}, which combines fragments of the {UD} and {UUDD} chains (Table 1, Figs. 5*b* and *c*). According to the authors (Koene *et al.*, 1998), the synthesis of $(tma)_5V_{18}O_{45}$ could not be repeated, which, along with complex configuration of the layer, suggests a metastable, intergrowth character of the crystals studied.

5.3. *Z-T structures*

This type of layered structure is built of {UuDd} chains joined into layers by tetrahedra sharing two corners with one and one corner with another chain. The zigzag {UuDd} chain is labeled as the Z chain and, in turn, the Z chain with corner-sharing tetrahedra on both sides T:{UuDd}:T is labeled as the ZT chain. A specific feature of the ZT chain is its flat configuration – the bases of all SPs and the base of T are approximately in the same plane in all known cases (Fig. 16). Nevertheless, ZT chains linked together may form a flat layer (Figs. 16*a*, *c*, *e* and *f*) or a step-like layer (Fig. 16*b* and 16*d*). There are two differentiating features of these layers: first the relative orientation of the linked chains and second which of the two possible T corners is shared with another ZT chain. The first defines four possible orientations of the chains in the layers marked with α, β, γ and δ in Table 10. The second determines the flat or step-like conformation. It is noteworthy that only the α and β orientation of the chains can form step-like layers denoted as α' and β'. Detailed topographical analysis and deduction of all possible Z-T layers is given by Zavalij *et al.* (1999). Thus, recently synthesized compounds represent five out of six simplest structures and only the δ layer has not yet been found.

The general formula of the layered structures constructed from the SP chain linked sharing terminal and bicoordinated corners of the SP base with tetrahedra is $V_{2(n+m)}O_{5n+4m}$, where n is the total number of SPs sharing neighboring edges and tetrahedra, and m is the number of SPs sharing opposite edges. However, only structures with $n = 2$ and $m = 1$ give V_3O_7 stoichiometry.

6. O structures

This section covers the class of vanadium oxide structures built only from octahedra, so is termed the O structure class. It is divided into three subclasses:

structures constructed from quadruple chains {Q};
structures from crossed quadruple chains {X};
structures containing single {o} and/or double {oo} chains of opposite edge-sharing octahedra.

6.1. *Q structures*

As follows from the name, the Q structures are built from quadruple chains of octahedra (Fig. 7*c*), which are described in §3.2. The Q chain has two types of octahedra with one and two terminal O atoms. These three terminal O atoms along with the bicoordinated oxygen which is already shared by two octahedra are used in different combinations to link the Q chains into various frameworks. To clarify further description of these links, these four corners are marked as shown in Fig. 17. The remaining O atoms are shared by three octahedra and do not bond externally.

Generally, six types of structures built from Q chains were found as listed in Table 11. The first type is just an

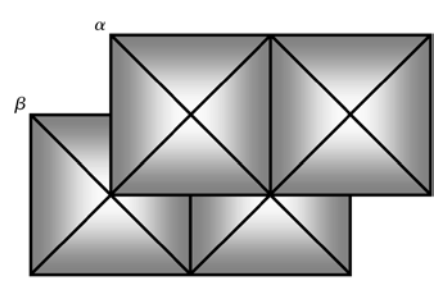

Fig. 17. Numeration of the shared corners in the {Q} chain.

Table 11. *Octahedral frameworks from Q chains*

Fig. 18	Formula	Compound	Space group	a (Å)	b (Å)	c (Å)	β (°)	Reference
(*a*)	{Q}	β-$AgVO_3$	*Cm*	18.11	3.58	8.04	104.4	(1)
		$Ag_{\sim 3}V_4O_{12}$	*Cm*	18.33	3.60	8.09	104.5	(2)
		β-SrV_2O_6	*Pcmn*†	12.53	3.68	9.67		(3)
		α-SrV_2O_6	*Pcmn*†	12.58	3.69	9.69		(3*a*)
		PbV_2O_6	*Pcmn*†	12.71	3.68	9.77		(3*b*)
(*b*)	({Q}.)	$Ag_{1.92}V_4O_{11}$	*C*2/*m*	14.51	3.58	9.56	128.7	(4)
		$Cu_{1.82}V_4O_{11}$	*Cm*	15.38	3.61	7.37	102.0	(5)
(*c*)	({Q}:)	$(tma)V_8O_{20}$	*C*2/*m*	23.65	3.59	6.32	103.1	(6)
(*d*)	({Q}|)	δ-$Na_xV_2O_5$, $x = 0.56$	*C*2/*m*	11.66	3.65	8.92	90.9	(7)
		τ-Na_xV_2O5, $x = 0.64$	*C*2/*m*	11.67	3.65	8.91	91.0	(8)
		δ-$Ag_{0.68}VO_5$	*C*2/*m*	11.74	3.67	8.74	90.5	(9)
		ε-$Cu_{0.828}V_2O_5$	*C*2/*m*	11.73	3.69	8.98	111.5	(10)
		ν-$Ca_{0.6}V_{2-x}O_5$	*C*2/*m*	11.81	3.71	9.27	101.9	(11)
		δ-$K_{0.486}V_2O_5$	*C*2/*m*	11.69	3.67	9.51	92.2	(12)
		$Tl_{0.5}V_2O_5$	*C*2/*m*	11.61	3.69	9.63	100.9	(13)
		$Ni_{0.25}V_2O_5.H_2O$	*C*2/*m*	11.76	3.65	10.36	95.0	(14)
		$Ca_{0.25}V_2O_5.H_2O$	*C*2/*m*	11.69	3.65	10.99	105.4	(14)
		$Ca_{0.72}V_2O_5.H_2O$	*C*2/*m*	11.68	3.65	11.02	105.0	(15)
	2({Q}|)	ρ-$K_{0.5}V_2O_5$	*Ccmm*†	11.61	3.68	18.63		(16)
(*e*)	[({Q}|).]	VO_2 (B)	*C*2/*m*	12.09	3.70	6.43	107.0	(17)
(*f*)	[({Q}|).({OO}.).]	V_6O_{13}	*C*2/*m*	11.92	3.68	10.14	100.9	(18)
			$P2_1/a$†	11.96	3.71	10.07	100.9	(19)
		$Li_xV_6O_{13}$	*C*2/*m*	11.86	3.66	10.91	100.4	(20)

† Converted to setting used in this work. (1) Rozier *et al.* (1996); (2) Drozdov *et al.* (1974); (3) Schnuriger *et al.* (1991); (3*a*) Karpov *et al.* (1989); (3*b*) Jordan & Calvo (1974); (4) Zandbergen *et al.* (1994); (5) Galy & Lavaud (1971); (6) Chirayil *et al.* (1997); (7) Kanke, Kato, Takayama-Muromachi & Isobe (1990); (8) Savariault *et al.* (1996); (9) Andersson (1965); (10) Ha-Eierdanz & Muller (1993); (11) Kutoglu (1983); (12) Oka *et al.* (1995*a*); (13) Ganne *et al.* (1992); (14) Oka *et al.* (1997); (15) Evans *et al.* (1994); (16) Kanke, Kato, Takayama-Muromachi, Isobe & Kasuda (1990); (17) Oka *et al.* (1993); (18) Dernier (1974) and Wilhelmi *et al.* (1971); (19) Kawada *et al.* (1978); (20) Bergström *et al.* (1997).

example of single-chain structures with the VO_3 composition. The two silver vanadates (Fig. 18*a*) are isostructural except for the silver occupation defect in the $Ag_{\sim 3}V_4O_{12}$ structure. The packing and conformation of the Q chains in the β-SrV_2O_6 structure are quite different, probably caused by the different content and type (charge) of the intercalated cations. Again notice that α- and β-modifications of the strontium metavanadate are essentially the same except for different labeling. Another metavanadate PbV_2O_6 also has the SrV_2O_6 structure type, which is known as β-SrV_2O_6. The repeat unit along the Q chain is 3.68 Å for the Sr and Pb, which is substantially greater than the 3.59–3.60 Å for the Ag compounds. The distribution of the weakest $V\cdots O$ bonds in Q chains for both Ag- and Sr-type structures is parallel, as shown in Fig. 8(*b*). However, in the β-SrV_2O_6 structure these weak bonds (2.56–2.73 Å) are substantially longer than the corresponding bonds in the Ag compounds (2.37–2.54 Å). The octahedra in the isolated Q chains have tetrahedral distortion in the β-SrV_2O_6 structure and both tetrahedral and square-pyramidal distortion in Ag compounds.

The next two types of structure (Fig. 18*b* and 18*c*) consist of Q chains that form a layer by sharing corners. The V_4O_{11} layer (Fig. 18*b*) is built from Q chains, which share only one β corner, whereas in the V_8O_{20} layer (Fig. 18*c*) Q chains are linked by sharing α and β corners with each other. This layer of two corners sharing Q chains was predicted by Rozier *et al.* (1996) for Ag compounds and was found later by Chirayil *et al.* (1997) in $(tma)V_8O_{20}$. The octahedra in the V_4O_{11} layer of one corner-sharing Q chain are distorted in the same manner as in the isolated chain of β-SrV_2O_6. However, in the V_8O_{20} layers of two corner-sharing chains only one octahedron has tetrahedral distortion, whereas the other with terminal oxygen has SP distortion as it takes place in an isolated chain of $Ag_xV_4O_{12}$.

The building block for the final three structures (Figs. 18*d–f*) is a layer of Q chains that share γ–δ edges with each other. The most commonly found type (Fig. 18*d*) with V_2O_5 composition contains ({Q}|) layers separated by metal ions and water of crystallization. The same layers, but sharing α and β corners with each other, form the three-dimensional framework of the VO_2 (B) structure (Fig. 18*e*), so that all octahedral corners are shared. The same ({Q}|) layer, sharing α and β corners with an alternating ({OO}.) layer, forms the V_6O_{13} framework (Fig. 18*f*). In this structure, as in the previous one, all octahedral corners are shared. The distortion of the octahedron in the presence of edge-sharing between the Q chains becomes more complicated and can be derived from either T or SP and in many cases it is between the T and SP. Moreover, some octahedra in the three-dimensional frameworks even approach regular polyhedra. These (Figs. 18*e* and 18*f*) are not strictly open frameworks. Nevertheless, the V_6O_{13} structure was found able to readily intercalate up to two and even three small Li ions per unit formula (Bergström *et al.*,

1997). Substantial changes of the octahedron distortion are observed while Li is intercalated into this framework. These changes lead to transformation of irregular V—O octahedral coordination into regular octahedral coordination that reflects reduction of the V oxidation states from +5 and +4 to +3.

There is a noticeable difference in the repeat distance along the Q chain (*b* cell parameter in Table 11), depending on whether the Q chains share edges or not. They are in the range 3.58–3.60 Å for separate and corner-sharing chains (Figs. 18*a–c*), except 3.68 Å for the β-SrV_2O_6 structure already mentioned, and 3.65–3.71 Å for edge-sharing chains (Figs. 18*d–f*).

The general stoichiometry of the structures constructed from the Q chains is $V_4O_{12-n/2}.mV_2O_5$, where n is the number of corners shared by the V_4O_{12} chain and m is the number of {OO} chains per Q chain. Thus, for structures containing only Q chains $m = 0$ and n can be 2, 4 or 8, giving the V_4O_{11}, V_4O_{10} and VO_2 compositions, respectively. The only structure with a mixed edge-sharing quadruple chain ($n = 8$) and a double chain ($m = 1$) yields the V_6O_{13} composition.

6.2. *X structures*

These structures with three-dimensional frameworks can be derived from the last two types of Q structures (Figs. 18*e* and 18*f*) by replacing the quadruple {Q} chain with a crossed quadruple {X} chain, so even the composition remains the same (VO_2 and V_6O_{13}; Table 12). Therefore, the stoichiometry of the X structures is described in the same way as the Q structures. However, there are substantial differences in the way the chains are linked to form the layer. In the case of Q structures, the chains share edges within the layers and two corners between the layers, whereas in X structures the chains share two corners in both directions (Figs. 19*a* and 19*b*). The distortion of the octahedron in the X structures is also complicated. The octahedron in VO_2 has one V—O bond just slightly shorter (1.83 Å) than the average single bond and therefore is close to a regular polyhedron. In contrast, the V_6O_{13} structure has trigonal-bipyramidal (type I) distortion in the {OO} chain and tetrahedral distortion in the X chain.

6.3. *o and oo structures*

These structures are built by corner-sharing {o} and/or {oo} chains (Figs. 7*d* and *e*) of the closest-packed O atoms with V in the octahedral sites. The V—O coordination polyhedron can be either a distorted or regular octahedron. However, here distortion is much less than in other vanadates: the short bond is not so short (1.7–1.8 Å) and the opposite weak bond is not so weak (2.0–2.2 Å). The first structure δ-VO_2 (Table 13) is the well known rutile framework formed by {o} chains (Fig. 20*a*).

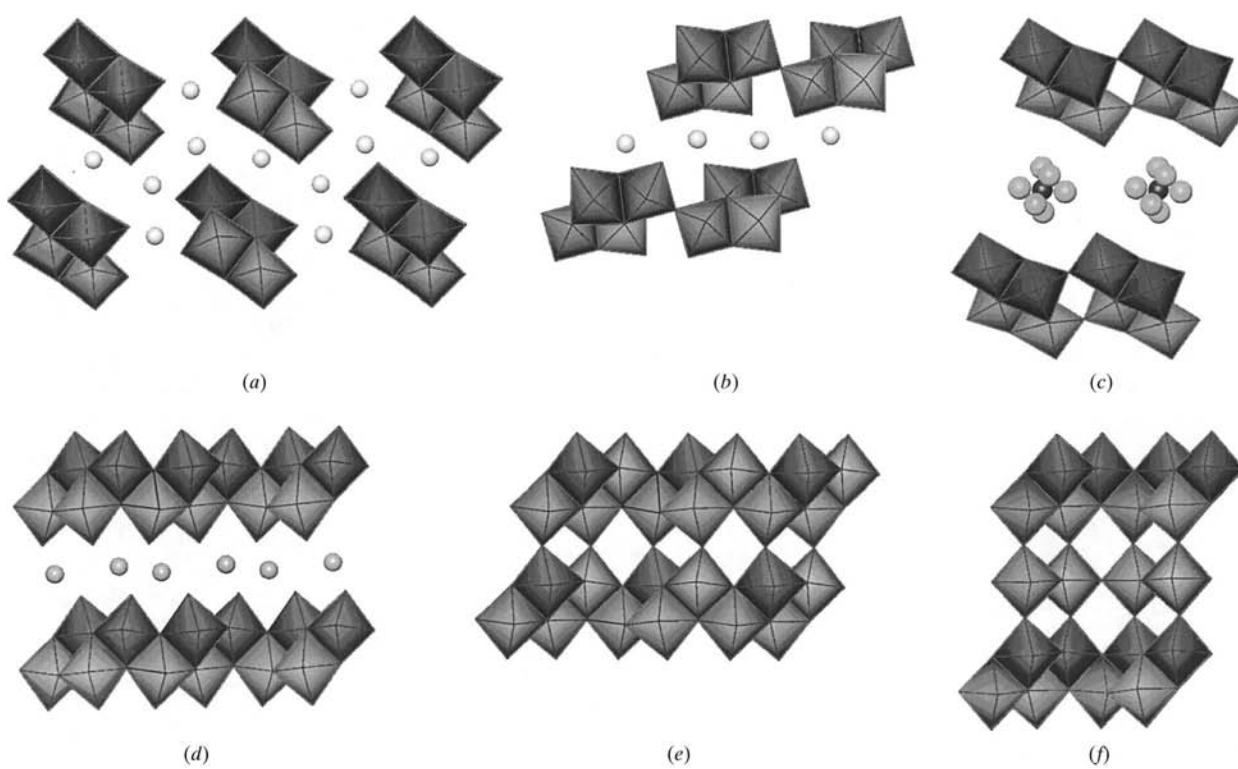

Fig. 18. Structures built up from Q-chains: (*a*) {Q}, (*b*) ({Q}.), (*c*) ({Q}:), (*d*) (Q), (*e*) [(Q).] and (*f*) [(Q):{OO}:].

Table 12. *Octahedral frameworks from X chains*

Fig. 19	Formula	Compound	Space group	a (Å)	b (Å)	c (Å)	Reference
(*a*)	[({X}:):]	VO_2 (A)	$P4_2/ncm$	8.48		7.62	Yao *et al.* (1994)
(*b*)	[({X}:):({OO}.):]	β-V_6O_{13}	*Cmma*	11.92	19.91	3.68	Ohno *et al.* (1985)

The second structure VO(OH) is constructed in the same way, but from {oo} double chains forming 2 × 1 tunnels (Fig. 20*b*). Next, the hollandite structure $M_xV_8O_{16}$ is also composed of {oo} double chains, but 2 × 2 tunnels are formed (Fig. 20*c*). 1 × 1 tunnels observed in the rutile and hollandite structures (Figs. 20*a* and 20*c*) are actually an arrangement of the closest-packed O atoms and therefore cannot be considered as tunnels from an intercalation point of view. However, 2 × 2 tunnels are large enough to host metal cations even as large as Ba, whereas in the case of 2 × 1 tunnels only H atoms from hydroxyl groups can fit in. The V oxidation states in this case can range from +4 in VO_2 to +3 in VO(OH). The last two layered structures are constructed from corner-sharing {oo} chains or alternating {o} and {oo} chains, as shown in Figs. 20(*d*) and 20(*e*), respectively.

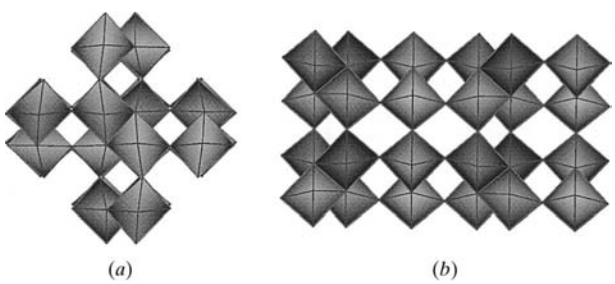

Fig. 19. Three-dimensional frameworks of X-chains: (*a*) [({X}:):] and (*b*) [({X}:):{OO}:].

This class is more common for Mn structures, since it is more stable with oxidation states in the range +3 to +4. Thus, even triple {ooo} and quadruple {oooo} chains were found in $Ba_{0.55}Mn_5O_{10}.nH_2O$ (Turner & Post, 1988), todorokite $(Na,K,Ca)_xMn_6O_{12}.nH_2O$ (Post & Bish, 1988) and $Rb_xMnO_2.nH_2O$ (Tamada & Yamamoto, 1986; Rziha *et al.*, 1996), which contain 3 × 2, 3 × 3 and 4 × 2 tunnels, respectively. The other example is the layered $LiMnO_2$ structure (Hoppe *et al.*, 1975; Croguennec *et al.*, 1995) built from {oo} chains sharing edges.

The stoichiometric formula for o structures is $V_nO_{2n+2-m/2}$, where n is order of the chain (number of single {o} chains) and m is the number of corners shared between the chains. Thus, m = 4 for three-dimensional frameworks (*a*, *b*, *c*) constructed from a single {o} chain (n = 1) and a double {oo} chain (n = 2), which yields VO_2 composition. Whereas, m = 2 for the layered compounds composed of double {oo} chains (n = 2) and a mixture of single {o} (n = 1) and double {oo} (n = 2) chains yielding V_2O_5 and V_3O_8 ($VO_3.V_2O_5$) compositions, respectively.

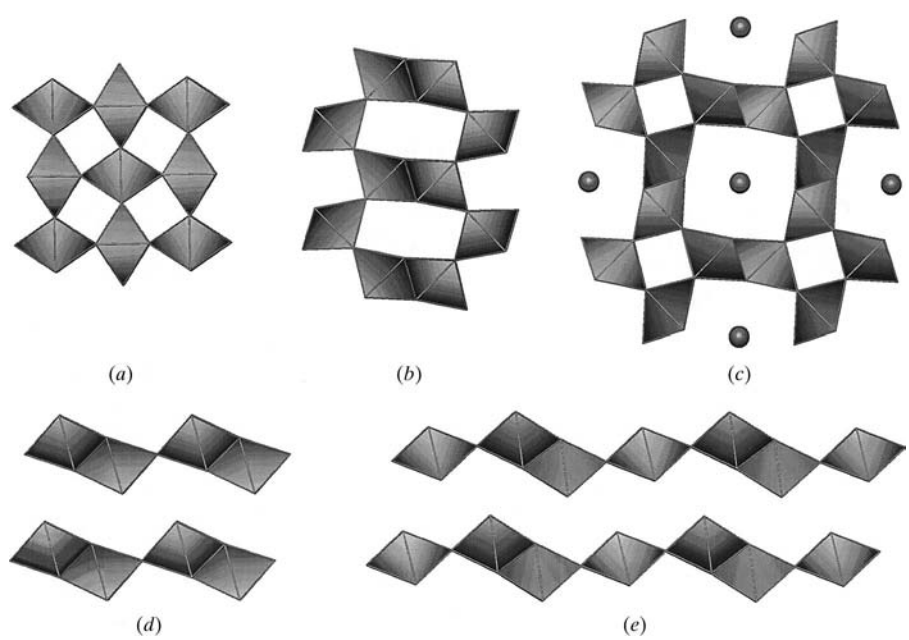

Fig. 20. Structures from {o} and {oo} chains: (*a*) [{o}.], (*b*) $[\{oo\}.]^{1\times2}$, (*c*) $[\{oo\}.]^{2\times2}$, (*d*) ({oo}.) and (*e*) ({oo}.{o}.)

Table 13. *Octahedral structures from {o} and {oo} chains*

Fig. 20	Formula	Compound	Space group	a (Å)	b (Å)	c (Å)	Angle (°)	Reference
(*a*)	[2{o}.]	δ-VO_2	*P*42/*mnm*	4.55		2.86		(1)
			Pnnm	4.51	4.63	2.87		(2)
			$P2_1/a$	5.38	4.54	2 × 2.88	β = 122.6	(3)
(*b*)	$[2\{oo\}.]^{1\times 2}$	VO(OH)	*Pbnm*	4.54	9.97	3.03		(4)
(*c*)	$[4\{oo\}.]^{2\times 2}$	$K_{2-x}V_8O_{16}$, x = 0, 0.2	*I*4/*m*	9.96		2.92		(5)
		$Tl_{2-x}V_8O_{16}$, x = 0.26		10.06		2.90		(5)
		$Bi_{2-x}V_8O_{16}$, x = 0.38		9.93		2.91		(6)
		$Ba_{2-x}V_8O_{16}$, x = 0.81		9.81		2.88		(7)
		$(Pb_{1.32}V_{0.35})V_8O_{16}$	*I*112/*m*	10.11	9.89	2.90	γ = 90.8	(8)
(*d*)	({oo}.)	$H_6V_4O_{10}$	*C*2/*m*	12.17	2.99	4.83	β = 98.3	(9)
(*e*)	({oo}.{o}.)	$H_{10}V_6O_{16}$	*C*2/*m*	19.64	2.99	4.83	β = 103.9	(9)

(1) Rogers (1993); (2) Range & Zintl (1983); (3) Longo & Kierkegaard (1970); (4) Evans & Mrose (1955); (5) Abriel *et al.* (1979); (6) Abraham & Mentre (1994); (7) Kanke *et al.* (1995); (8) Mentre & Abraham (1996); (9) Evans & Mrose (1960).

7. O-SP structures

Structures built from a combination of octahedra and square pyramids are divided into two groups. The first major group unites structures constructed from quadruple octahedral {Q} chains and square pyramidal {UD} chains. The other is represented by only two structures.

7.1. *Q-UD structures*

The large variety of Q-UD structures (Table 14), where Q and UD chains are mixed, is the result of the availability in Q chains of four types of corners for sharing, which are labeled as α, β, γ and δ in Fig. 17. In contrast the {UD} chain has only one such corner, the apex of SP is rarely shared. The two types of layered

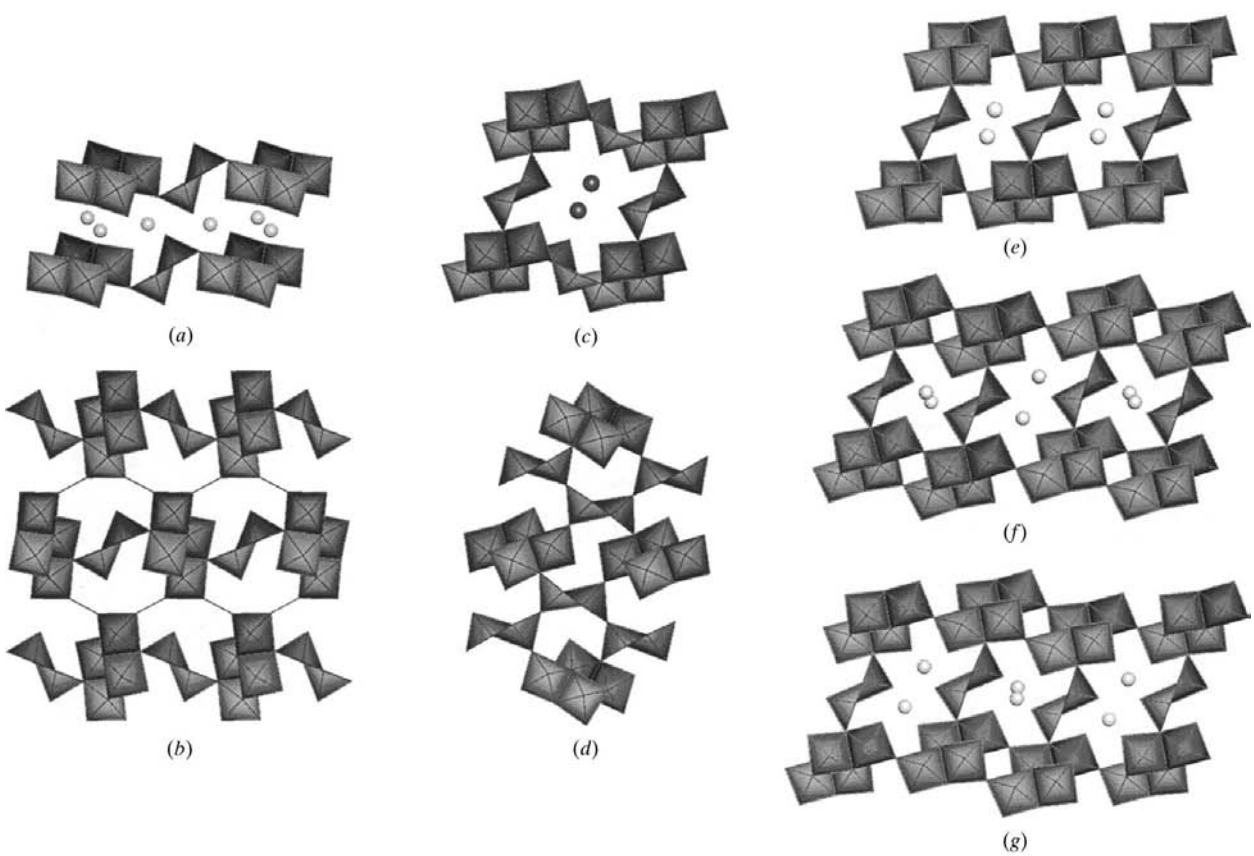

Fig. 21. Structures combining Q and UD chains: (*a*) β({Q}.{UD}.) ≡ β(QUD), (*b*) δ'({Q}.{UD}.) ≡ δ'(QUD), (*c*) [(QUD)|{UD}^{a}|] (^{a} disordered), (*d*) [*(.3{UD}$_*$).2{Q}.], (*e*) [(QUD).], (*f*) [(QUD):(QUD).] and (*g*) [(QUD):(QUD).(QUD).].

Table 14. *Q-UD frameworks*

Fig. 21	Formula	Compound	Space group	a (Å)	b (Å)	c (Å)	β (°)	Reference
(*a*)	β(QUD) ≡ β({Q}.{UD}.)	$Li_{1.2}V_3O_8$	$P2_1/m$	6.60	3.56	11.86	107.7	(1)
(*b*)	δ'(QUD) ≡ δ'({Q}.{UD}.)	$V_3O_7.H_2O$	*Pnma*	16.93	3.64	9.36		(2)
			Pnma	16.88	3.64	9.34		(3)
(*c*)	[δ(QUD)|{UD}|]≡ δ[({Q}|{UD}|).{UD}.]	$Ba_{0.4}V_3O_8(VO)_{0.4}.H_2O$	$P2_1/m$	9.44	3.63	10.15	102.1	(4)
(*d*)	[{Q}.(.{UD}*)*]	V_4O_9	*Pnma*	17.93	3.63	9.40		(5)
(*e*)	[(QUD).] ≡ [({Q}.).{UD}.]	β-$Ag_{0.333}V_2O_5$	*C*2/*m*	15.39	3.62	10.07	109.7	(6)
		β-$Cu_{0.55}V_2O_5$	*Cm*	15.25	3.62	10.10	106.9	(7)
		$Na_{0.333}V_2O_5$	*C*2/*m*	15.45	3.62	10.09	109.6	(8), (9)
		$Na_{0.287}V_2O_5$	*C*2/m	16.44	3.61	10.09	109.6	(10)
		β-$Li_{0.3}V_2O_5$	*C*2/*m*	15.38	3.60	10.03	110.7	(11)
		β'-$Li_{0.48}V_2O_5$	*C*2/*m*	15.27	3.62	10.10	107.7	(12)
		$K_{0.33}V_2O_5$	*C*2/*m*	15.34	3.61	10.04	109.2	(13)
		$Cu_{0.261}V_2O_5$	*C*2/*m*	15.24	3.62	10.10	107.3	(14)
		β-$Pb_{0.333}V_2O_5$	*C*2/*m*	15.46	3.65	10.12	109.2	(15)
(*f*)	[(QUD):(QUD).] ≡ [({Q}:{Q}.).2{UD}.]	β-$Li_xV_{12}O_{29}$, x = 1.5	*C*2/*m*	28.22	3.61	10.12	102.1	(16)
		x = 2.1		28.04	3.62	10.13	100.1	
		$Cu_xV_{12}O_{29}$, x = 1.2	*C*2/*m*				100.0	(17)
		x = 1.5		28.01	3.62	10.14	99.7	
		x = 1.7					99.5	
(*g*)	[(QUD):(QUD).(QUD).] ≡ [({Q}:{Q}.{Q}.).3{UD}.]	β'-$Li_xV_9O_{22}$, x = 1.2	$P2_1/m$	21.82	3.61	10.10	105.3	(18)
		x = 1.7		21.61	3.62	10.12	102.7	

(1) de Picciotto *et al.* (1993); (2) Oka *et al.* (1990); (3) Weeks *et al.* (1999); (4) Oka *et al.* (1995); (5) Wilhelmi & Waltersson (1970); (6) Ha-Eierdanz & Muller (1993); (7) Galy *et al.* (1970); (8) Khamaganova & Trunov (1988); (9) Wadsley (1955); (10) Kobayashi (1979); (11) Hardy *et al.* (1964); (12) Galy *et al.* (1971); (13) Ozerov *et al.* (1957); (14) Kato *et al.* (1989*b*); (15) Kato *et al.* (1990); (16) Kato & Takayama-Muromachi (1987*a*); (17) Kato *et al.* (1989*a*); (18) Kato & Takayama-Muromachi (1987*b*).

Q-UD structures (Figs. 21*a* and *b*) differ in which corner of the Q chain is shared, β in the case of LiV_3O_8 and δ in $V_3O_7.H_2O$. These ({Q}.{UD}.) layers, termed for simplicity QUD, differ also in their stacking – β layers are separated by Li ions, whereas δ layers interact by H bonds, which link β and γ corners of the Q chains. The next structure, $Ba_{0.4}V_3O_8(VO)_{0.4}.H_2O$ (Fig. 21*c*) is built with δ(QUD) layers, but linked together by sharing edges with other UD chains. The exact structure of this framework is not completely clear owing to the 40% occupation disorder of the edge-sharing UD chain. However, this δ layer differs from that in $V_3O_7.H_2O$ by the orientation of the UD chain. Therefore, the layer in $V_3O_7.H_2O$ is denoted as a δ'(QUD) layer in contrast to δ(QUD) in the Ba compound. The latter case is very common for Q-UD structures so δ may be omitted for simplicity.

The V_4O_9 structure (Fig. 21*d*) is built from Q and UD chains in a very specific way, unlike the other Q-UD structures. The UD chains are linked to each other by sharing a corner of the base on one side and an apex on the other side. This unusual (*{UD}.) layer shares basic and apical SP corners with β and δ corners of Q chains producing a three-dimensional network.

The final three structures $M_xV_2O_5$, $M_xV_{12}O_{29}$ and $M_xV_9O_{22}$ (Figs. 21*e–g*) consist of δ(Q.UD) layers, which are stacked in much the same manner. Thus, in the V_2O_5 framework (Fig. 21*e*) the β corners of the Q chain are shared [(QUD).], in the $V_{12}O_{29}$ framework (Fig. 21*f*) each pair of Q-UD layers is joined by α and β corners, whereas only β corners are shared between pairs [(QUD):(QUD).], and finally in the V_9O_{22} framework (Fig. 21*g*) the same pair of layers (QUD):(QUD) alternates with a single (QUD) layer by sharing only β corners [(QUD):(QUD).(QUD).]. As follows from Figs. 21(*e*)–(*g*), an alternative description of Q-UD structures can be given as layers of one or two corner-sharing Q chains linked with {UD} chains, as indicated in Table 14. However, the (QUD) layer is more generalized and therefore primarily used.

In all the Q-UD structures there is an additional O atom opposite the V═O apex of SP or, in other words, SP attempts to complete the V coordination polyhedron to an octahedron. However, the V*sp*···O distances are greater than the 2.6 Å limit considered for including atoms in V polyhedra. Moreover, forcing octahedral coordination would make interpretation and description of the vanadium oxide structure types more complicated and inconsistent with each other. However, this approach was used by Galy *et al.* (1996) to describe the $Li_xV_{3(1+n)}O_{8+7n}$ series of structures composed of QUD layers. On the other hand, the weak $V_O\cdots O$ bonds in the octahedra are in the range 2.2–2.4 Å, which is significantly below the 2.6 Å limit for V*sp*···O distances. The distortion of the octahedra is unambiguous square-pyramidal in all QUD layers.

The stoichiometry of the Q-UD structures (except the unusual V_4O_9 structure that does not belong to these series) is $V_6O_{16-n/2}$, where n is the number of corners that the Q chain shared with other layers. Thus, n = 0 for layered V_3O_8 structures, n = 2 for V_2O_5 and n = 3 for $V_{12}O_{29}$. The last most complex layer is composed of two-

Table 15. *Structures from mixed O and SP pairs or chains*

Fig. 22	Formula	Compound	Space group	a (Å)	b (Å)	c (Å)	β (°)	Reference
(*a*)	({UDO}.)	KV_3O_8	$P2_1/m$	7.64	8.38	4.98	96.9	(1)
		TlV_3O_8	$P2_1/m$	7.78	8.42	4.99	96.5	(2), (3)
		$NH_4V_3O_8$	$P2_1/m$	7.86	8.41	5.00	96.4	(4)
		CsV_3O_8	$P2_1/m$	8.18	8.52	4.99	95.5	(1)
(*b*)	[.{⟨OO⟩:}.2{UU}*{O.}.{UD}*]	V_3O_7	$C2/c$	21.92	3.68	18.34	95.6	(5)

(1) Evans & Block (1966); (2) Benchrifa *et al.* (1990); (3) Sokolova *et al.* (1983); (4) Range *et al.* (1990); (5) Waltersson *et al.* (1974).

corner-sharing QUD layers and two three-corner-sharing QUD layers (n = 8/3), which yields $V_2O_5.2V_{12}O_{29}$ or the V_9O_{22} composition. The QUD layers can share up to four corners (n = 4), which leads to the hypothetical V_3O_7 structure first proposed by Galy *et al.* (1996).

7.2. *O-UD structures*

The two types of O-UD structures contain V_3O_8 layers (Fig. 22*a*) and V_3O_7 three-dimensional frameworks (Fig. 22*b*). The V_3O_8 layers are found in potassium, thallium, ammonium and caesium compounds (Table 15), and consist of corner-sharing chains made of octahedra and a UD pair sharing edges in the following sequence {UD|O|DU|O|}. The octahedron is only slightly distorted and the sixth weakly bonded O atom (V···O = 2.1–2.3 Å) is shared with two SPs. On the other hand, SP has an additional V···O contact with length 2.9 Å, which is much over the 2.6 Å limit. The {UDO} chains share corners to form a ({UDO}.) layer with metal ions intercalated between them.

The three-dimensional framework of the V_3O_7 structure (Fig. 22*b*) is formed from two types of octahedral chains and two types of square pyramidal chains, which share corners with each other. The octahedral chains are built from a single octahedron {O.} and an edge-sharing pair of octahedra {⟨OO⟩:}, which share only corners along the chain. The octahedral chains share all their corners with two types of square pyramidal chains {UD} and {UU}. The first, {UD}, shares both terminal corners of the base of the SP and both apical corners, whereas the second {UU} shares two corners of the base and only one apical corner. This is the only case where a {UU} chain has been found. However, the two UU chains are in such an orientation that the oxygen from one chain would complete the SP from another chain to give an octahedron. Thus, the well known {Q} chain can be formed by approaching two antiparallel {UU} chains (Fig. 8*b*) to each other. However, the V*sp*···O contacts are 2.74 and 3.56 Å in length and the last is far above the 2.6 Å limit.

The general stoichiometry in this case cannot be expressed in any reasonable way because of the quite different structure type of the only two members in this subclass.

8. O-T structures

This class of vanadium oxide structure is built of octahedra and tetrahedra. The division into subclasses was made by octahedral building blocks: separate polyhedra, chains and layers.

8.1. *O-T structures with separate octahedra*

This type of structure with separate or corner-sharing octahedra consists of three known members (Table 16).

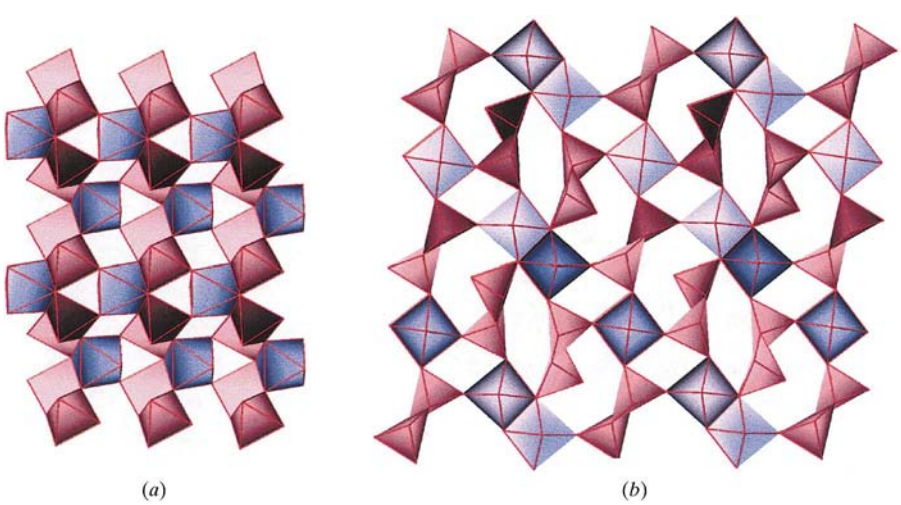

Fig. 22. Structures from O and SP pairs or chains: (*a*) ({UDO}.) and (*b*) [.{⟨OO⟩:}.2{UU}*{O.}.{UD}*].

Table 16. *Frameworks from mixed single O and T*

Fig. 23	Formula	Compound	Space group	a (Å)	b (Å)	c (Å)	β (°)	Reference
(*a*)	({O.}.T.)	$Sr_2V_3O_9$	$I2/a$	6.93	16.25	7.26	115.8	(1)
(*b*)	(O.⟨T.T.⟩.)	BaV_3O_8	$P2_1$	7.44	5.55	8.20	107.2	(2)
(*c*)	(O.{2T.}.)	(phen)V_3O_7 ($V_3O_7N_2$)	$P2/c$	9.59	10.06	15.01	98.8	(3)

(1) Feldmann & Mueller-Buschbaum (1995); (2) Oka *et al.* (1995*b*); (3) Duan *et al.* (1995).

The first, $Sr_2V_3O_9$ (Fig. 23*a*) has a chain of corner-sharing octahedra as a skeleton. There are two types of tetrahedra: one additionally links each pair of octahedra along the chain, the other joins the chains into a layer. Each tetrahedron shares two corners, while the octahedra share all six corners and so the structural chemical formula is $Sr_2V^{IV}O(V^{V}O_4)_2$. This corner-sharing chain of octahedra with a $\cdots V{=}O\cdots V{\equiv}O\cdots$ bond sequence along the chain is very similar to that found in $VO(CH_3COO)_2$ (Weeks *et al.*, 1999) (Fig. 9*b*), where acetate ions play a similar role to the VO_4 group in the title structure. However, acetate ions link pairs of V atoms only along the chain. The $\cdots V{=}O\cdots V{=}O\cdots$ feature is also found in many other compounds such as α-V_2O_5, treated here as a UD structure so the weak bond is ignored.

Next, the BaV_3O_8 structure (Fig. 23*b*) consists of separate octahedra and the V_2O_7 pyrovanadate group a pair of corner-sharing tetrahedra, which are joined into a double sheet layer by sharing corners with the octahedra. The pyrovanadate group and octahedron share five of six corners, with the sixth O atom remaining terminal. Thus, the structural formula is $BaV^{IV}O(V^{V}_2O_7)$.

The last structure, (phen)V_3O_7 (Fig. 23*c*), is the first layered structure with bidentante organic ligands (Oka *et al.*, 1995*b*). The octahedra share three corners with tetrahedra, two external neighboring corners are occupied with N atoms from the chelate ligand and one corner remains terminal directing inside the layer. The tetrahedra sharing two corners with each other form a zigzag chain. As in previous cases, this structure can be considered as a double sheet layer. The structural formula is $(phenV^{IV}O)(V^{V}O_3)_2$.

The stoichiometry of the O-T structure $V_{1+n}O_{3+2n+m/2}$ depends on the T:O ratio (n) and the number of unshared corners (m). Thus, $n = 2$ and $m = 4$ for $Sr_2V_3O_9$ and (phen)V_3O_7, giving V_3O_9 ($V_3O_7N_2$ for the organic complex), and $n = 2$ and $m = 2$ for BaV_3O_8.

8.2. *W-T structures with chains of octahedra*

The building block in these structures is a wave-like chain {W} (Fig. 7*f*) of octahedra sharing semi-adjacent edges. This chain can also be derived from the closest-packed double chain {oo} by removing each third octa-

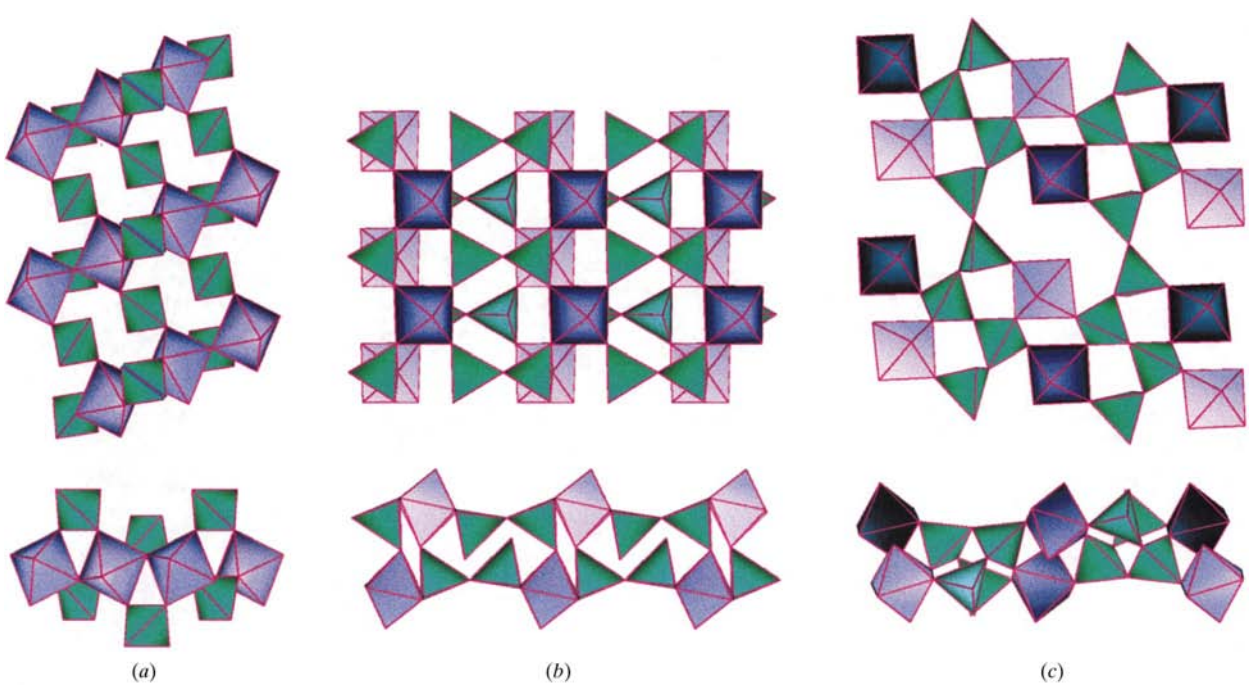

Fig. 23. Structures from octahedra and tetrahedra: (*a*) ({O.}.2T.), (*b*) (O..⟨T.T⟩..) and (*c*) (O..{2T.}.).

Table 17. *Structures from mixed {W} chains and T*

Fig. 25	Formula	Compound	Space group	a (Å) α (°)	b (Å) β (°)	c (Å) γ (°)	Reference
(*a*)	({W}:T.)	NiV_2O_6	$P\bar{1}$	7.13 90.2	8.82 94.1	4.79 102.2	(1)
	[({W}:T.).]	$FeV_2O_6H_{0.5}$	$P2_12_12_1$	4.89	9.55	8.79	(2)
(*b*)	[({W}:2T.).]	β-MgV_3O_8	$C2/m$	10.30	8.53 119.5	7.74	(3)
(*c*)	(..U|{W}:T.)	σ-$Zn_{0.25}V_2O_5.H_2O$	$P\bar{1}$	10.61 90.7	8.03 91.1	10.77 90.1	(4)

(1) Mueller-Buschbaum & Kobel (1991); (2) Muller *et al.* (1979); (3) Saux & Galy (1973); (4) Oka *et al.* (1996).

hedron in each row. There are four known structures constructed with {W} chains (Table 17).

The first two, MV_2O_6, consist of {W} chains linked by tetrahedra into layers (Fig. 24*a*) with an octahedron to tetrahedron ratio of 2:1. Thus, the composition of the layer is V_3O_9 or V_2O_6. An almost flat surface layer is formed by octahedral faces and tetrahedral corners. However, despite the same stoichiometry of the NiV_2O_6 and $FeV_2O_6H_{0.5}$ (not counting H atoms), these two structures are quite different. The Ni compound is composed of $V_2O_6^{2-}$ layers where Ni atoms occupy octahedral sites between the layers. Whereas in the same layer of the Fe compounds 1/3 of the V atoms are substituted with Fe atoms, so that the actual stoichiometry of the layer is FeV_2O_9. These layers share all surface corners to form a three-dimensional framework yielding the FeV_2O_6 composition.

The next structure, MgV_3O_8 (Fig. 24*b*), is also composed of {W} chains and tetrahedra. However, in this case the octahedron to tetrahedron ratio is 2:2, giving a layer composition of V_4O_{10}. These layers shown in Fig. 24(*b*) are joined into a three-dimensional framework by sharing corners: octahedra with octahedra and tetrahedra with tetrahedra, so that the overall composition is V_4O_8. However, half of the V atoms in octahedral sites are substituted with Mg atoms in a disordered manner to give the MgV_3O_8 composition. Another feature, which differentiates the V_4O_8 layer from the previous V_3O_9, is the orientation of the {W} chain, so that both octahedral and tetrahedral terminal O atoms form the surface of the layer.

The last structure, $Zn_{0.25}V_2O_5.H_2O$ (Fig. 24*c*), is again composed of {W} chains, but linked into the layer by tetrahedra and square pyramids. Nevertheless, it is almost identical to the previous V_4O_{10} layer and can be derived from it by some slight deformation, in a way that some of the tetrahedra are converted to square pyramids. However, in this case the layers are separated by Zn ions and water molecules, and do not share corners.

The stoichiometry of the W-T layers is $V_{2+n}O_{8+n-m/2}$, where n is the total number of T and SP, and m is the number of interlayer shared corners (both per two

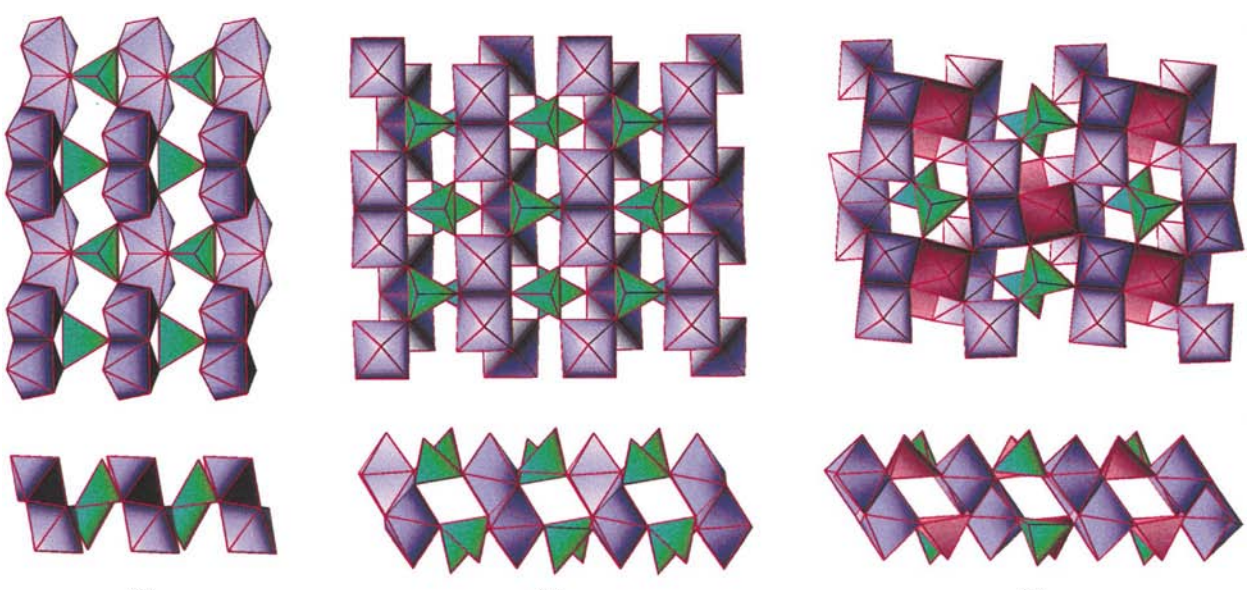

Fig. 24. W-T layers: wave-like O chains linked with T and SP: (*a*) ({W}:T.), (*b*) ({W}:2T.) and (*c*) (..U|{W}:T.).

Table 18. *Examples of vanadium oxide clusters*

Fig. 26	Cluster	Compound	Reference
(*a*)	$V_{12}O_{32}$	$(Ph_4P)_4[CH_3CN.V_{12}O_{32}].3CH_3CN.4H_2O$	(1)
(*b*)	$V_{18}O_{42}$	$Na_{12}[V_{18}O_{42}].24H_2O$	(2)
		$Na_6[H_9V_{18}O_{42}(VO_4)].21H_2O$	(3)
(*c*)	$V_{15}O_{36}$	$K_5[H_2V_{15}O_{36}(CO_3)].15H_2O$	(4)
		$Li_7[H_2V_{15}O_{36}(CO_3)].\sim 39H_2O$	(5)
		$(tma)_6[V_{15}O_{36}(Y)].4H_2O$ (Y = Cl, Br)	(5)
		$(NH_4)_3Na_7[V_{15}O_{36}(Cl)].30H_2O$	(6)
		$[NH_3(CH_2)_8NH_3]_3[V_{15}O_{36}(Cl)].6NH_3.3H_2O$	(7)
(*d*)	$V_{22}O_{54}$	$(N(C_2H_5)_4)_6[HV_{22}O_{54}(ClO_4)]$	(8)
		$(tma)_8[V_{22}O_{54}(CH_3COO)].4H_2O$	(9*a*)
		$(tma)_8[V_{22}O_{54}(MoO_4)]Cl$	(9*b*)
(*e*)	$V_{18}O_{47}$	$(NH_4)_8[V_{18}O_{38}(OH)_9(VO_3)]$.$11H_2O$	(10)
(*f*)	$V_{10}O_{28}$	$((CH_3)_3CNH_3)_6[V_{10}O_{28}].8H_2O$	(11)
		$(enH_2)_3[V_{10}O_{28}].2H_2O$	(12)
		$[Li(H_2O)_4]_2(tma)_4[V_{10}O_{28}].4H_2O$	(13)
		$Na_4(tma)_2[V_{10}O_{28}].20H_2O$	(14)
		$[CH_3(CH_2)_{11}N(CH_3)_3]_4[H_2V_{10}O_{28}].4H_2O$	(15)
		$(tma)_4[H_2V_{10}O_{28}].CH_3COOH.2.8H_2O$	(16)

(1) Day *et al.* (1989); (2) Meicheng *et al.* (1985); (3) Müller & Döring (1991); (4) Yamase & Ohtaka (1994); (5) Müller *et al.* (1990); (6) Shao *et al.* (1990); (7) Drezen *et al.* (1998); (8) Müller *et al.* (1991); (9*a*) Chirayil *et al.* (1998*b*); (9*b*) Nazar (1998); (10) Müller *et al.* (1988); (11) Averbuch-Pouchot (1994); (12) Ninclaus *et al.* (1996); (13) Zavalij, Whittingham *et al.* (1997); (14) Zavalij *et al.* (1997*b*); (15) Janauer *et al.* (1997); (16) Pecquenard *et al.* (1998).

octahedra). Thus, $n = 1$ for Ni and Fe structures, but m is 0 and 6, giving V_3O_9 (or V_2O_6) and V_3O_6 (Fe substitute 1/3 of V) compositions, respectively. The following Mg and Zn structures have two T and SP every two octahedra ($n = 2$), while m is 4 and 0 yielding V_4O_8 (Mg substitute 1/4 of V) and V_4O_{10} compositions.

8.3. *o-T structure with a layer of octahedra*

$BaV_7O_{16}.nH_2O$, recently discovered by Wang *et al.* (1998), is the one representative of this type of layer. It crystallizes in space group $P4_2/m$ with $a = 6.16$ and $c = 21.52$ Å. Its layer consists of two sheets of edge-sharing octahedra, as shown in Fig. 25. Two of the five octahedral sites in the layer are not occupied. Four empty sites, two from the lower and two from the upper sheet, are linked by a tetrahedrally coordinated V atom. Thus, the symbol for this layer is $((OoOee)_2..T..)$. Despite its unique position in the family of the octahedral structures, this double sheet layer can be described by two SP sheets linked together by weak V···O bonds, which shows a relationship with ude layers. As can be easily seen from Fig. 25, a single sheet of square pyramids consists of edge-sharing chains, where two SPs share neighboring edges and one SP shares the opposite edges of the base {UuU}. These chains only share corners yielding the ({UuU}.) layer related to UuDd structures (see §5.3). On the other hand, this SP sheet is also related to ude layers (§4.3) with 2/5 of the sites empty and with the $(\{uuuee\}^3)$ symbol. The latter allows to apply a stoichiometric formula for ud layers V_nO_{2n+m}, so $n = 3$ and $m = 2$ with an extra V atom in the tetrahedral cavity result in a V_7O_{16} ($2\ V_3O_8$.V) composition.

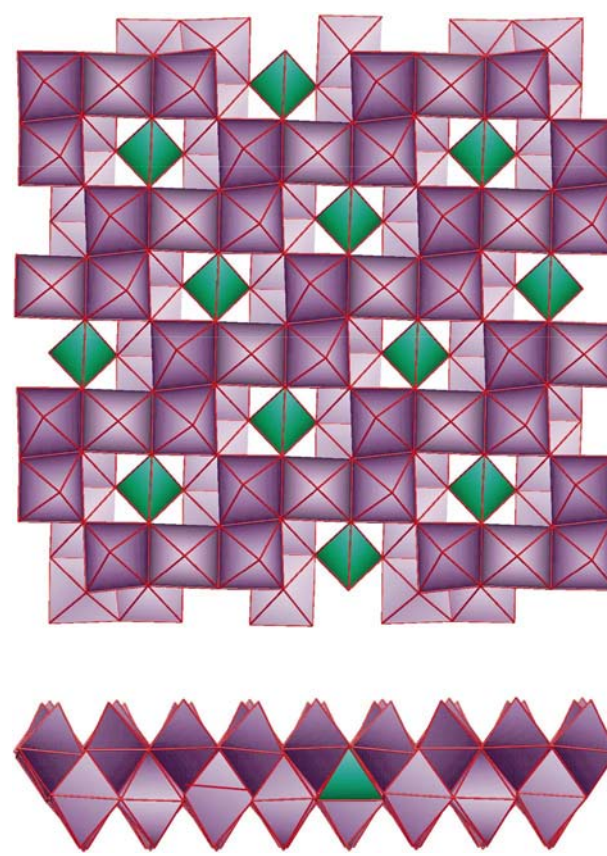

Fig. 25. Octahedral double sheets layered with inserted tetrahedra $((OoOee)_2.T)$.

9. Clusters

This chapter describes some of the vanadium oxide clusters (Table 18). The first two clusters are built in a similar manner, $[V_{12}O_{32}]$ (Fig. 26*a*) and its completed version $[V_{18}O_{42}]$ (Fig. 26*b*), and have open and closed cavities, respectively. $[V_{12}O_{32}]$ hosts the organic molecule acetonitrile in its mouth, whereas $[V_{18}O_{42}]$ can be either empty $[V_{18}O_{42}]$ or filled $[H_9V_{18}O_{42}(VO_4)]$. Another structural motive was found in the next two clusters $[V_{15}O_{36}]$ (Fig. 26*c*) and $[V_{22}O_{54}]$ (Fig. 26*d*) with different size of cavities. The first, $[V_{15}O_{36}]$ holds such small inorganic anions as Cl^-, Br^- and CO_3^{2-}, while another $[V_{22}O_{54}]$ hosts bigger inorganic ions ClO_4^- or MoO_4^{2-} and the organic ion CH_3COO^-. The $[(Cl)V_{15}O_{36}]$ cluster is often found as large hexagonal crystals when chloride ions are present in the reaction media. Another $[V_{18}O_{47}]$ cluster (Fig. 26*e*) hosting a disordered VO_4 group is an example of mixed octahedra, square pyramids and tetrahedra. Fig. 26(*f*) depicts the very common decavanadate cluster that consists of the closest-packed O atoms with V atoms occupying the octahedral sites. Finally, the very common decavanadate cluster $[V_{10}O_{28}]$ is constructed with ten octahedra in the same way as shown in Fig. 26(*f*).

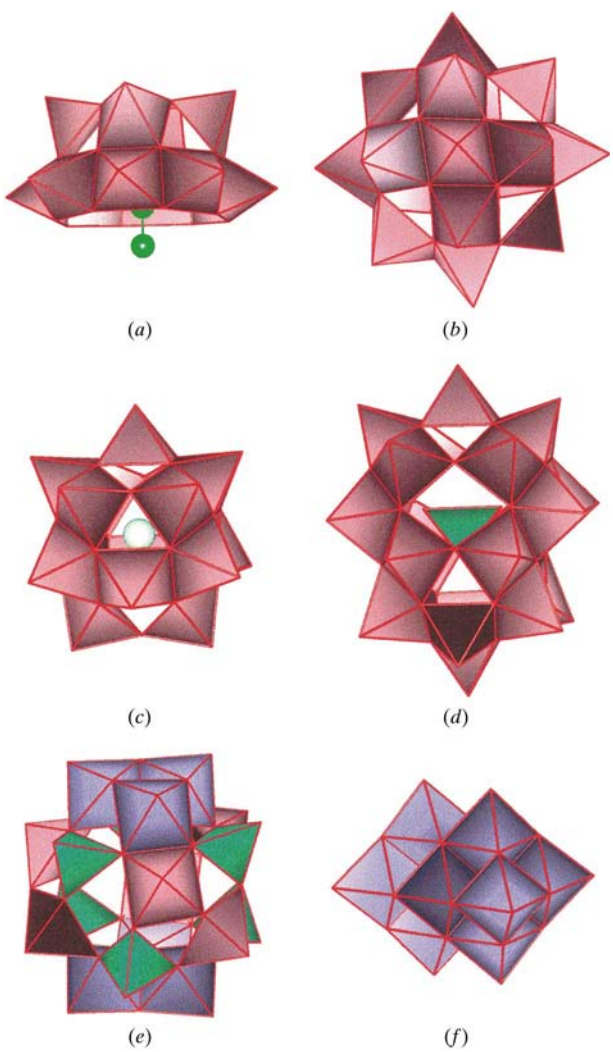

Fig. 26. Most common vanadium clusters: (*a*) $[V_{12}O_{32}]$, (*b*) $[V_{18}O_{42}]$, (*c*) $[V_{15}O_{36}]$, (*d*) $[V_{22}O_{54}]$, (*e*) $[V_{18}O_{47}]$ and (*f*) $[V_{10}O_{28}]$.

As Table 18 shows, the charge of the cluster can vary because of the different oxidation states of V atoms, *e.g.* -5 in $K_5[H_2V_{15}O_{36}(CO_3)].4H_2O$ compared with -7 in $Li_7[H_2V_{15}O_{36}(CO_3)].39H_2O$. The charge of the cluster can also be reduced by attached H atoms, *e.g.* -4 in $(tma)_4[H_2V_{10}O_{28}].CH_3COOH.2.8H_2O$ compared with -6 in $[Li(H_2O)_4]_2(tma)_4[V_{10}O_{28}].4H_2O$.

It is clear from Fig. 26 that the formation of the clusters, despite their finite size, is governed by the same principles as the formation of other vanadium oxide structures with an open framework. Thus, the clusters shown in Figs. 26(*a*) and 26(*b*) are built with fragments of the {uu} chain, which buckle into a ring because the relative rotations between the equally directed SP groups have the same sense. The clusters shown in Figs. 26(*c*) and 26(*d*) are constructed in a similar manner, but from both U and u square pyramids. Therefore, the $V_{22}O_{54}$ cluster (Fig. 26*d*) can be described as a barrel formed with four bent ⟨UUUU⟩ fragments that share corners with each other and are covered at the top and bottom with 2 ⟨uuu⟩ arcs.

10. Discussion

The classification summarized in Table 19 splits up vanadium oxide frameworks into five classes by polyhedron types and into 14 subclasses by the structural units present. In total this review covers approximately 60 different structure types of vanadium oxide with vanadium in oxidation states greater than +3 with tetrahedral, square pyramidal and octahedral coordination. Those with only tetrahedral coordination were excluded from the review, as they are traditional valence compounds, whose structures decompose when the vanadium oxidation state changes. Structures with trigonal bipyramidal coordination are not classified as a separate class since they are represented by only two types of chains, which are parental for square pyramidal layers and are discussed there. The cluster compounds are described here only for completeness; they can be divided into cluster classes in a similar manner. Thus, the $V_{12}O_{32}$ and $V_{18}O_{42}$ clusters can be described with opposite edge-sharing SPs, whereas $V_{15}O_{36}$ and $V_{22}O_{54}$ are formed mostly by adjacent edge-sharing SPs. Another cluster, $V_{10}O_{28}$, belongs to octahedral formation and the last $V_{18}O_{47}$ cluster combines all types of polyhedra together – tetrahedra, square pyramids and octahedra.

The proposed notation can also be applied to frameworks with other metal oxides, such as molyb-

Table 19. *Classification of vanadium oxide frameworks*

Class (polyhedra type)	Subclass (structural unit type)		Dimension	No. of types	Description
SP	1	UD	One-dimensional, two-dimensional	3+2†	Layers of corner-sharing UD chains
	2	UD pipes	One-dimensional, three-dimensional	2	Tunnel structure from corner-sharing UD chains
	3	ude	Two-dimensional	5 + 1	Layers of edge-sharing SPs
SP + T	4	U-T	Two-dimensional	3	Separate SP and T
	5	UD-T	Two-dimensional	5	UD blocks and T
	6	ZT	Two-dimensional	6	Zigzag UuDd chain and T
O	7	Q	One-dimensional, two-dimensional, three-dimensional	5 + 1	Corner- and edge-sharing quadruple chains
	8	X	Three-dimensional	2	Corner-sharing crossed quadruple chains
	9	o-oo	Two-dimensional, three-dimensional	5	Closest packed single and double o chains shared corners
O + SP	10	Q-UD	Two-dimensional, three-dimensional	7	Corner-sharing Q and UD chains
	11	O-UD	Two-dimensional, three-dimensional	2	Separate or corner-sharing O and UD blocks or chains
O + T	12	O-T	One-dimensional, two-dimensional	3 + 1	Separate or corner-sharing O and T
	13	W-T	Two-dimensional, three-dimensional	3	Wave-like O chains and T
	14	oe-T	Two-dimensional	1	Double sheet layer of edge-sharing O with inserted T

† Chain types are separated by '+'

denum and tungsten, which are built mostly from distorted octahedra; however, tetrahedral and pentagonal coordination can be found as well. Thus, the structure of molybdenum oxide M_xMoO_3 (Guo *et al.*, 1994, 1995) is built from {OO} chains, which share corners and form hexagonal tunnels in a three-dimensional framework. The same type of chain exists as a separate structural unit in the $[WO_2(O_2)H_2O].nH_2O$ (n = 0, 2) structures, where one corner of an octahedron is occupied by an O_2 peroxo group (Pecquenard, Castro-Garcia *et al.*, 1998). On the other hand, the classification cannot be simply extended from vanadium oxide to molybdenum and tungsten oxide frameworks because of their more complex and slightly different crystal chemistry, *e.g.* the square pyramidal coordination is not common.

Topography of the vanadium oxide frameworks results in 11 types of stoichiometry related to 14 subclasses, as shown in Table 20. The O-UD cannot be expressed by simple formula because two known representatives are complex enough and quite different. A few more subclasses are described by the same formula. This is why the number of general stoichiometric formulae is less than the number of structure types. The general stoichimetric formula is a function of two (rarely one or three) integer numbers. The variation of these integers would generate, as it might seem, numerous compositions of the vanadium oxides in the range from VO_2 to VO_3. However, only 13 compositions (Table 21) have been found among the described vanadium oxides. The most common and most represented is V_2O_5 followed by VO_2, VO_3, V_3O_8 and V_3O_7, and finally V_6O_{13} and V_4O_9. The others are represented with only one structure type or even one compound. Table 21 presents the distribution of the stoichiometry (O:V ratio) among the structural subclasses where the dimension of the framework is denoted with breaks used in the symbolic formula: {} – chain, () – layer and [] – three-dimensional framework. The classes and subclasses in Table 21 are approximately ordered from SP-T to O according to the average coordination number of vanadium. The conclusions below follow from Table 21.

Table 21 shows that one-dimensional structures have only the VO_3 composition in the whole range of coordination numbers from 4 in tetrahedral chains (not shown) to 6 in pure octahedral structures.

The three-dimensional structures have a well defined area where they can exist – left bottom corner of the table. In other words, three-dimensional frameworks fall in the VO_2–V_6O_{13} stoichiometric range with a very low O:V ratio for O and O-T structures, but this range extends up to V_2O_5 composition when octahedra are mixed with SPs, as in the Q-UD structures. There are two exceptions: in $Cs_{0.35}V_3O_7$ UD pipes from a three-dimensional framework are composed with SPs due to the single case of sharing corners by three UD chains, and in $BaV_7O_{16}.nH_2O$ the oe-T structure with low O:V ratio is constructed mostly from octahedra.

Table 20. *General stoichiometric formula of vanadium oxide frameworks*

Class	Subclass	General formula	n = number of	m = number of	Stoichiometry of known compounds
SP	UD	V_nO_{2n+1}	Chains sharing corners		$n = 1$ VO_3 (chain); $n = 2$ V_2O_5 (layer)
	UD-pipes				$n = 2$ V_2O_5; $n = 3$ V_3O_7
	ud	V_nO_{2n+m}	Occupied sites	Vacant sites	$m = 0$, $n = 1$ VO_2; $m = 1$: $n = 2$ V_2O_5 (UD layers), $n = 3$ V_3O_7, $n = 4$ V_4O_9
SP + T	U-T	$V_{(n+m)}O_{(3n+5m/2)}$	SPs	T	$n = 1$: $m = 2$ V_3O_8, $m = 4$ V_5O_{13}; $n = 3$, $m = 2$ V_5O_{14}
	UD-T	$V_{2(n+m)}O_{5(n+m)}$	SP units	T	V_2O_5
	Z-T	$V_{2(n+m)}O_{5n+4m}$	T + corner SPs	Middle SPs	$n = 2$, $m = 1$ V_3O_7
O	Q	$V_4O_{12-n/2}.mV_2O_5$	Shared corners	O chains	$m = 0$: $n = 0$ V_4O_{12}, $n = 2$ V_4O_{11}, $n = 4$ V_4O_{10}, $n = 8$ V_4O_8; $m = 1$, $n = 8$ V_6O_{13}
	X				$n = 8$: $m = 0$ V_4O_8, $m = 1$ V_6O_{13}
	o	$VO_{2+n/2}$	Unshared corners		$n = 0$ VO_2, $n = 1$ V_2O_5, $n = 1{,}2$ V_2O_5 + VO_3 = V_3O_8
O + T	O-T	$V_{1+n}O_{3+2n+m/2}$	T per O	Unshared corners	$n = 2$: $m = 2$ V_3O_8, $m = 4$ V_3O_9
	W-T	$V_{2+n}O_{8+n-m/2}$	T per 2O	Interlayer shared corners	$n = 1$, $m = 0$ V_3O_9; $n = 2$: $m = 0$ V_4O_{10}, $m = 4$ V_4O_8
	oe-T	$V_{n+k}O_{2n+m}$	Occupied sites	Vacant sites	$n = 6$, $m = 4$, $k = 1$ V_7O_{16} (k is number of inserted T)
O +SP	Q-UD	$V_6O_{16-n/2}$	Corners shared between layer		$n = 0$ V_3O_8, $n = 2$ V_2O_5, $n = 3$ $V_{12}O_{29}$, $n = (2 + 3 + 3)/3$ V_9O_{22} (only for QUD structures)

The layered structures are the most common and have the widest ranges of existence. Thus, the structures are layered in the presence of octahedral coordination only at a high O:V ratio ranging from V_2O_5 up to VO_3. The single exception for V_2O_5 stoichiometry is a three-dimensional framework [(QUD).]. However, when the square-pyramidal coordination is the highest (*i.e.* SP and SP-T structures), the layered frameworks result in the whole stoichiometric range, except for the VO_3 composition. Nevertheless, some O-T structures are composed of VO_3 layers, but these structures can be considered as a three-dimensional framework with mixed metals as well.

Fig. 27 depicts the distribution of vanadium oxidation states as a function of stoichiometry. The upper bold line delimits the highest possible vanadium oxidation states (y) and can be expressed as $y_{max} = \min(2x, 5)$, where x is the O:V ratio and 5 is the maximal possible oxidation state for vanadium. The lower border of the shaded area indicates the most common minimal vanadium oxidation states for the reviewed compounds. It can be expressed as $y_{min} = 2x - 2/3$. It does not mean that there are no compounds below that line. As shown in Fig. 27, there are a few compounds below that line up to the $y = 2x - 1$ dashed line. Again this figure depicts only an area where the structures described in this review exist. However, structures with vanadium in oxidation state +3 and below would expand the area, but these structures are somewhat different. The conclusion that follows from Fig. 27 is that vanadium oxidation states in the open framework structures can be reduced from the maximal possible value for 2/3 or in rare cases for 1. Obviously this limitation also reflects the amount of lithium ions that can be intercalated without collapsing the structure.

Finally, this review helps in the understanding of vanadium oxide structures, deduces new structure types, explains intercalation properties and helps in the search

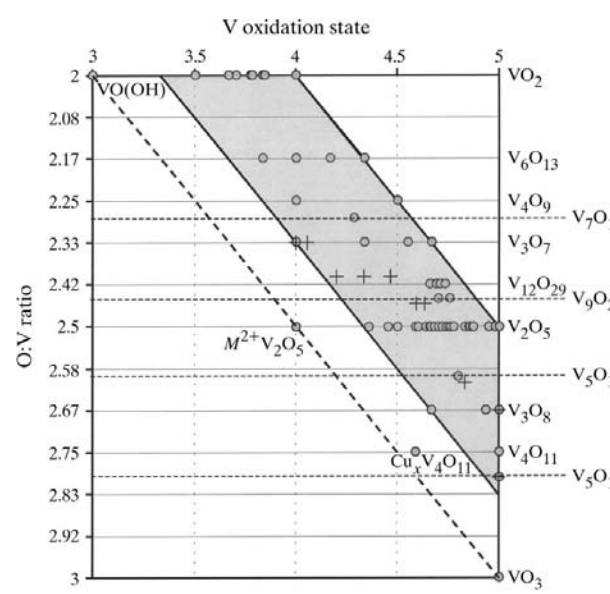

Fig. 27. Oxidation states of vanadium as a function of stoichiometry. Clusters are shown with plus signs.

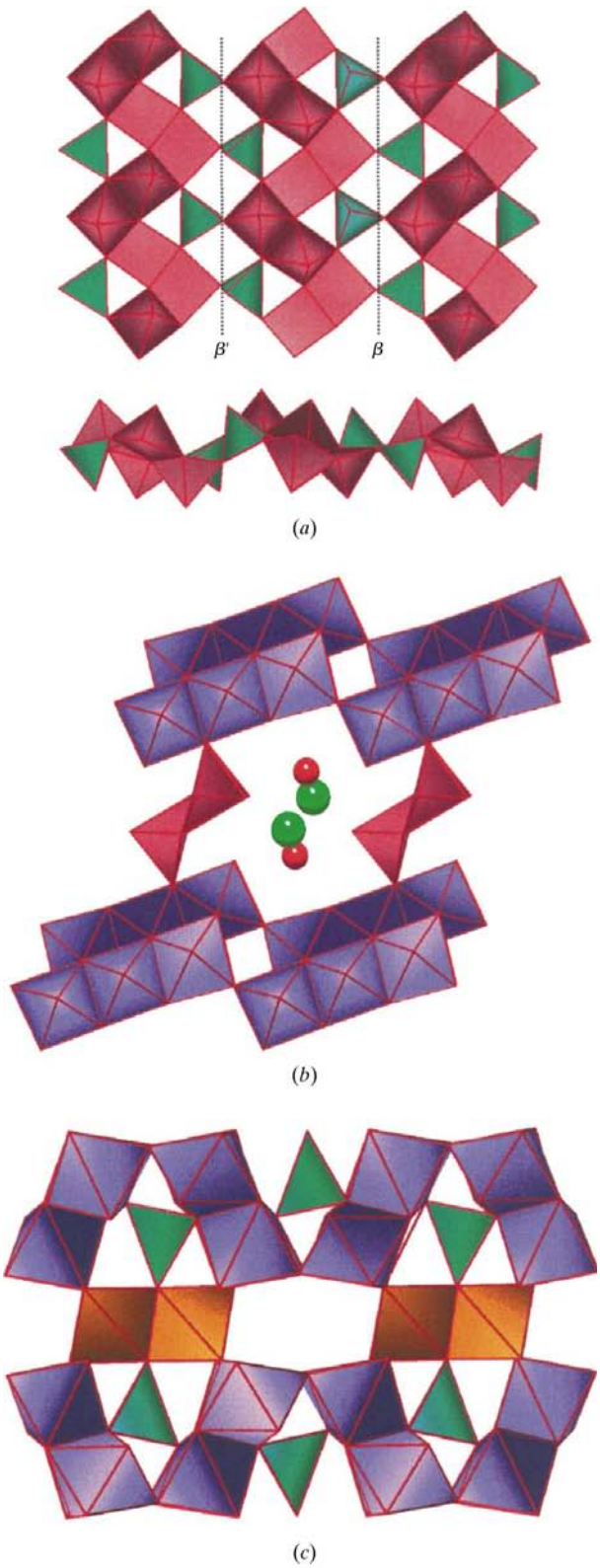

Fig. 28. New types of the vanadium oxide structures: (*a*) $(tma)_2[Co(H_2O)_4]V_{12}O_{28}$, (*b*) $SrV_{12}O_{27}.3H_2O$ and (*c*) α-CoV_3O_8.

for new materials with particular properties. The principles can be used to solve nonconventional crystal structures, such as $(tma)V_3O_7$ (Zavalij *et al.*, 1997*a*), which was solved from poor-quality X-ray powder data only after a review of the known vanadium oxide structures and possible vanadium coordination. Another example is the determination of the structure of $(en_2Ni)V_6O_{14}$ (Zavalij *et al.*, 1999), for which an ordered model was obtained using a structural knowledge of the possible structures of V_6O_{14} layers.

11. Recently published new vanadium oxide structures

While this manuscript was under review more vanadium oxide structures with open frameworks were solved and the most interesting of them are described briefly below.

The structure presented by Jacobson (1998), $(tma)_2[Co(H_2O)_4]V_{12}O_{28}$ or $(tma)_2[Co(H_2O)_4](V_3O_7)_4$ (Fig. 28*a*), belongs to the SP + T class and Z-T subclass (see §5.3). This Z-T structure is the first representative in the series of V_3O_7 layers with two types of links (β and β') between ZT chains. Its symbolic formula is β,β'-({UuDd}:2T.) or β,β'-({Z}:2T.). The presence of two types of the chain links is caused, as could be expected, by two types of intercalated ions tma^+ and $[Co(H_2O)_4]^{2+}$. In this structure as well as in all simple ZT structures (Table 10) only one symmetrically independent chain is present, however, in this case the symmetry of the chain is lowered to $\wp 1$ from $\wp 2_1$.

An interesting $SrV_{12}O_{27}.3H_2O$ or $Sr(V_4O_9)_3.3H_2O$ structure (Fig. 28*b*) published by Kato & Kante (1998*b*) belongs to the O + SP class and is closely related to Q-UD structures. However, the quadruple chain is substituted with a similarly constructed hexamer chain (H). The symbolic formula [({H}.{UD}.):] or alternative [({H}:).{UD}.] denotes the sharing of two corners between H chains. The latter fact makes this H-UD structure a structural analog to the hypothetical V_3O_7 structure, [({Q}.{UD}.):] (see §7.1). This structure type might be considered as a first member of a new H-UD subclass or still can be put into the same Q-UD subclass, which however has to be termed multi-O-UD.

The α-CoV_3O_8 structure (Fig. 28*c*) solved by Oka *et al.* (1998) belongs to the W-T subclass in the O + T class (see §8.2). This structure has a disordered distribution of Co and V atoms in an octahedral site and is isotypical to ZnV_3O_8 (Lloyd & Galy, 1973), however, with ordered Zn atoms and therefore is not included in this review as having a mixed-metal framework. This structure is composed of a new type of W-T layer (Fig. 28*c*), which is closely related to that in NiV_2O_6 and $FeV_2O_6H_{0.5}$ (Fig. 25*a*). It is composed of W chains alternating along the layers, so they share corners in the orientation where the octahedral faces are parallel to the surface of the layer. The tetrahedra additionally bond these chains. The symbolic formula is [({W}.T.)].B|B.], which along with Fig. 28(*b*) depicts a three-dimensional connection of the

Table 21. *Stoichiometry of vanadium oxide frameworks versus structure types*

Class	Subclass	Stoichiometry and O:V ratio												
		VO_2 2	V_6O_{13} 2.17	V_4O_9 2.25	V_7O_{16} 2.29	V_3O_7 2.33	$V_{12}O_{29}$ 2.42	V_9O_{22} 2.44	V_2O_5 2.5	V_5O_{13} 2.6	V_3O_8 2.67	V_4O_{11} 2.75	V_5O_{14} 2.8	VO_3 3
SP + T	U–T			()						()	()		()	
	UD–T								()					
	Z–T					()								
SP	ud	()	()	()		()								{}
	UD								()					{}
	UD pipes					[?]			()					
O + T	O–T										()			() { }
	W–T	[]							()					()
	oe–T				(?)									
O + SP	O–UD					[]					()			
	Q–UD			[]			[]	[]	[]		()			
O	Q	[]	[]						()			()		{}
	X	[]	[]											
	o	[]							()		()			{}

layers by a pair of trigonal bipyramids (B) occupied by vanadium.

More papers propose a new discussion and new compounds with known structure type. Thus, Ueda (1998) gave a review of spin-gap systems in the (2{UD}.) layer (α'-NaV_2O_5, CaV_2O_5, MgV_2O_5), in the ({UD}.{DU}.) layer (γ-LiV_2O_5) and in the (⟨UD⟩.2T.) layer (CsV_2O_5).

Hagrman *et al.* (1998) obtained $VO_2.1/2H_2O$ with a (ud) layered structure (see §4.3) – an analog of $Li_xV_{2-y}O_{4-y}.H_2O$ (Chirayil *et al.*, 1996*b*) without inserted Li.

A new quinuclidinium vanadate $[N(C_7H_{14})]V_4O_{10}$ (Riou *et al.*, 1998) was found to be the second representative of ({UUDD}.) layers.

Kato & Kante (1998*a*) discussed order–disorder and twinning in $Sr_{0.5}V_2O_5$ as alternating in the stacking of ({Q}|) layers.

This work was supported by the National Science Foundation through grant DMR-9810198 and CRDF grant UCI-305. We also thank Dr Emil Lobkovsky from Cornell University, NY, USA, for the use of the Cambridge Structural Database.

References

Abraham, F. & Mentre, O. (1994). *J. Solid State Chem.* **109**, 127–133.
Abriel, W., Rau, F. & Range, K. J. (1979). *Mater. Res. Bull.* **14**, 1463–1468.
Addison, A. W., Rao, T. N., Reedijk, J., van Rijn, J. & Verschoor, G. C. (1984). *J. Chem. Soc. Dalton Trans.* pp. 1349–1356.
Ahmed, F. R. & Barnes, W. H. (1963). *Can. Miner.* **7**, 713–726.
Allen, F. H. & Kennard, O. (1993). *Chem. Des. Autom. News*, **8**, 31–37.
Andersson, S. (1965). *Acta Chem. Scand* **19**, 1371–1375.
Averbuch-Pouchot, M.-T. (1994). *Eur. J. Solid State Chem.* **31**, 557–565.
Avtamonova, N. V., Trunov, V. K. & Bezrukov, I. Ya. (1990). *Izv. Akad. Nauk SSSR Neorg. Mater.* **26**, 346–349.
Bachmann, H. G., Ahmed, F. R. & Barnes, W. H. (1961). *Z. Kristallogr.* **115**, 110–131.
Benchrifa, R., Leblanc, M. & De Pape, R. (1990). *Acta Cryst.* C**46**, 177–179.
Bergström, Ö., Gustafsson, T. & Thomas, J. O. (1997). *Acta Cryst.* C**53**, 528–530.
Bjoernberg, A. & Hedman, B. (1977). *Acta Chem. Scand. Ser. A*, **31**, 579–584.
Bouloux, J. C. & Galy, J. (1973*a*). *Acta Cryst.* B**29**, 269–275.
Bouloux, J. C. & Galy, J. (1973*b*). *Acta Cryst.* B**29**, 1335–1338.
Bouloux, J. C. & Galy, J. (1976). *J. Solid State Chem.* **16**, 385–388.
Bouloux, J. C., Milosevic, I. & Galy, J. (1976). *J. Solid State Chem.* **16**, 393–398.
Carpy, A. & Galy, J. (1971). *Bull. Soc. Fr. Mineral. Crystallogr.* **94**, 24–29.
Carpy, A. & Galy, J. (1975). *Acta Cryst.* B**31**, 1481–1482.
Cava, R. J., Santoro, A., Murphy, D. W., Zahurak, S. M. & Fleming, R. M. (1986). *J. Solid State Chem.* **65**, 63–71.
Chen, R., Zavalij, P. Y. & Whittingham, M. S. (1999). *J. Mater. Chem.* pp. 93–100.
Chirayil, T., Zavalij, P. Y. & Whittingham, M. S. (1996*a*). *J. Electrochem. Soc.* **143**, L193–L195.
Chirayil, T., Zavalij, P. Y. & Whittingham, M. S. (1996*b*). *Solid State Ion.* **84**, 163–168.
Chirayil, T., Zavalij, P. Y. & Whittingham, M. S. (1997). *J. Mater. Chem.* **7**, 2193–2195.
Chirayil, T., Zavalij, P. Y. & Whittingham, M. S. (1998*a*). *Chem. Mater.* **10**, 2629–2640.
Chirayil, T., Zavalij, P. Y. & Whittingham, M. S. (1998*b*). *Acta Cryst.* C**54**, 1441–1444.
Christian, H. P. & Mueller-Buschbaum, H. (1974). *Z. Naturforsch. Teil B*, **29**, 713–715.
Cocciantelli, J. M., Gravereau, P., Doumerc, J. P., Pouchard, M. & Hagenmuller, P. (1991). *J. Solid State Chem.* **93**, 497–502.
Corman, C. R., Geiser-Bush, K. M., Rowley, S. P. & Boyle, P. D. (1997). *Inorg. Chem.* **36**, 6401–6408.
Croguennec, L., Deniard, P., Brec, R. & Lecerf, A. (1995). *J. Mater. Chem.* **5**, 1919–1925.

Day, V. W., Klemperer, W. G. & Yaghi, O. M. (1989). *J. Am. Chem. Soc.* **111**, 5959–5961.
Dernier, P. D. (1974). *Mater. Res. Bull.* **9**, 955–964.
Dhaussy, A.-C., Abraham, F., Mentre, O. & Steinfink, H. (1996). *J. Solid State Chem.* **126**, 328–335.
Dickens, P. D., French, S. J., Hight, A. T. & Pye, M. F. (1979). *Mater. Res. Bull.* **14**, 1295–1299.
Drezen, T., Joubert, O., Ganne, M. & Brohan, L. (1998). *J. Solid State. Chem.* **136**, 298–304.
Drozdov, Y. N., Kuz'Min, E. A. & Belov, N. V. (1974). *Kristallografiya*, **19**, 65–69.
Duan, C. Y., Tian, Y. P., Lu, Z. L. & You, X. Z. (1995). *Inorg. Chem.* **34**, 1–2.
Enjalbert, R. & Galy, J. (1986). *Acta Cryst.* C**42**, 1467–1469.
Evans, H. T. (1960). *Z. Kristallogr.* **114**, 257–277.
Evans, H. T. & Block, S. (1966). *Inorg. Chem.* **5**, 1808–1814.
Evans, H. T. & Brusewitz, A. M. (1994). *Acta Chem. Scand.* **48**, 533–536.
Evans, H. T. & Mrose, M. E. (1955). *Am. Mineral.* **40**, 861–874.
Evans, H. T. & Mrose, M. E. (1960). *Am. Miner.* **45**, 1144–1166.
Evans, H. T., Post, J. E., Ross, D. R. & Nelen, J. A. (1994). *Can. Mineral.* **32**, 339–351.
Feldmann, J. & Mueller-Buschbaum, H. (1995). *Z. Naturforsch. Teil B*, **50**, 43–46.
Galy, J. (1992). *J. Solid State Chem.* **100**, 229–245.
Galy, J. & Carpy, A. (1975). *Acta Cryst.* B**31**, 1794–1795.
Galy, J., Darriet, J. & Hagenmueller, P. (1971). *Rev. Chim. Miner.* **8**, 509–522.
Galy, J. & Lavaud, D. (1971). *Acta Cryst.* B**27**, 1005–1009.
Galy, J., Lavaud, D., Casalot, A. & Hagenmueller, P. (1970). *J. Solid State Chem.* **2**, 531–543.
Galy, J., Savariault, J.-M. & Roucau, C. (1996). *Aust. J. Chem.* **49**, 1009–1018.
Ganne, M., Jouanneaux, A., Tournoux, M. & Le Bail, A. (1992). *J. Solid State Chem.* **97**, 186–198.
Guo, J.-D., Whittingham, M. S. & Zavalij, P. Y. (1994). *Eur. J. Solid State Inorg. Chem.* **31**, 833–842.
Guo, J.-D., Zavalij, P. Y. & Whittingham, M. S. (1995). *J. Solid State Chem.* **117**, 323–332.
Ha-Eierdanz, M.-L. & Muller, U. (1992). *Z. Anorg. Allg. Chem.* **613**, 63–66.
Ha-Eierdanz, M.-L. & Muller, U. (1993). *Z. Anorg. Allg. Chem.* **619**, 287–292.
Hagrman, D. E., Haushalter, R. C. & Zubieta, J. (1998). Private communication.
Hagrman, D., Zubieta, J., Warren, C. J., Meyer, L. M., Treacy, M. M. J. & Haushalter, R. C. (1998). *J. Solid State Chem.* **138**, 178–182.
Hardy, A., Galy, J., Casalot, A. & Pouchard, M. (1964). *Bull. Soc. Chim. Fr.* **1964**, 2808–2811.
Hoppe, R., Brachtel, G. & Jansen, M. (1975). *Z. Anorg. Allg. Chem.* **417**, 1–10.
Huang, S. D. & Shan, Y. (1998). *Chem. Commun.* pp. 1069–1070.
Jacobson, A. J. (1998). *MRS 1998 Fall Meeting*, Boston, USA. Abstract of papers, pp. 544–545.
Janauer, G. G., Dobley, A. D., Zavalij, P. Y. & Whittingham, M. S. (1997). *Chem. Mater.* **9**, 647–649.
Jordan, B. D. & Calvo, C. (1974). *Can. J. Chem.* **52**, 2701–2704.
Kanke, Y., Kato, K., Takayama-Muromachi, E. & Isobe, M. (1990). *Acta Cryst.* C**46**, 536–538.
Kanke, Y., Kato, K., Takayama-Muromachi, E., Isobe, M. & Kosuda, K. (1990). *Acta Cryst.* C**46**, 1590–1592.
Kanke, Y., Takayama-Muromachi, E., Kato, K. & Kosuda, K. (1995). *J. Solid State Chem.* **115**, 88–91.
Karpov, O. G., Simonov, M. A., Krasnenko, T. I. & Zabara, O. A. (1989). *Sov. Phys. Crystallogr.* **34**, 838–839.
Kato, K., Kante, Y., Oka, Y. & Yao, T. (1998*a*). *Z. Kristallogr.* **213**, 399–405.
Kato, K., Kante, Y., Oka, Y. & Yao, T. (1998*b*). *Z. Kristallogr.* **213**, 532–536.
Kato, K., Kosuda, K., Koga, T. & Nagasawa, H. (1990). *Acta Cryst.* C**46**, 1587–1590.
Kato, K. & Takayama, E. (1984). *Acta Cryst.* **40**, 102–105.
Kato, K. & Takayama-Muromachi, E. (1987*a*). *Acta Cryst.* C**43**, 1447–1451.
Kato, K. & Takayama-Muromachi, E. (1987*b*). *Acta Cryst.* C**43**, 1451–1454.
Kato, K., Takayama-Muromachi, E. & Kanke, Y. (1989*a*). *Acta Cryst.* C**45**, 1841–1844.
Kato, K., Takayama-Muromachi, E. & Kanke, Y. (1989*b*). *Acta Cryst.* C**45**, 1845–1847.
Kawada, I., Ishii, M., Saeki, M., Kimizuka, N., Nakano-Onoda, M. & Kato, K. (1978). *Acta Cryst.* B**34**, 1037–1039.
Khamaganova, T. N. & Trunov, V. K. (1988). *Z. Neorg. Khim.* **34**, 295–298.
Kobayashi, H. (1979). *Bull. Chem. Soc. Jpn*, **52**, 1315–1320.
Koene, B. E., Taylor, N. J. & Nazar, L. F. (1998). Private communication.
Konnert, J. A. & Evans, H. T. (1987). *Am. Mineral.* **72**, 637–644.
Kutoglu, A. (1983). *Z. Kristallogr.* **162**, 263–272.
Leonowicz, M. E., Johnson, J. W., Brody, J. F., Shannon, H. F. & Newsam, J. M. (1985). *J. Solid State Chem.* **56**, 370–378.
Liu, G. & Greedan, J. E. (1995). *J. Solid State Chem.* **115**, 174–186.
Lloyd, D. J. & Galy, J. (1973). *Cryst. Struct. Commun.* **2**, 209–211.
Longo, J. M. & Kierkegaard, P. (1970). *Acta Chem. Scand.* **24**, 420–426.
Meicheng, S., Yongjian, Z. & Yougi, T. (1985). *J. Mol. Sci.* **5**, 1–8.
Mentre, O. & Abraham, F. (1996). *J. Solid State Chem.* **125**, 91–101.
Millet, P., Satto, C., Sciau, P. & Galy, J. (1998). *J. Solid State Chem.* **136**, 56–62.
Mueller-Buschbaum, H. & Feldmann, J. (1996). *Z. Naturforsch.* **51**, 489–492.
Mueller-Buschbaum, H. & Kobel, M. (1991). *Z. Anorg. Allg. Chem.* **596**, 23–28.
Müller, A. & Döring, J. (1991). *Z. Anorg. Allg. Chem.* **595**, 251–274.
Muller, J., Joubert, J. C. & Marezio, M. (1979). *J. Solid State Chem.* **27**, 367–382.
Müller, A., Kirckemeyer, E., Penk, M., Rohlfing, R., Armatage, A. & Bögge, H. (1991). *Angew. Chem. Int. Ed. Engl.* **30**, 1674–1677.
Müller, A., Penk, M., Krickemeyer, E., Bögge, H. & Walberg, H. J. (1988). *Angew. Chem.* **100**, 1787–1788.
Müller, A., Penk, M., Rohlfing, R., Kirckemeyer, E. & Döring, J. (1990). *Angew. Chem. Int. Ed. Engl.* **29**, 926–927.
Murphy, D. W., Christian, P. A., DiSalvo, F. J. & Waszczak, J. V. (1979). *Inorg. Chem.* **18**, 2800–2803.
Nazar, L. F. (1998). Private communication.

Nazar, L. F., Koene, B. E. & Britten, J. F. (1996). *Chem. Mater.* **8**, 327–329.
Ninclaus, C., Riou, D. & Férey, G. (1996). *Acta Cryst.* C**52**, 512–514.
Ohno, T., Nakamura, Y. & Nagakura, S. (1985). *J. Solid State Chem.* **56**, 318–324.
Oka, Y., Tamada, O., Yao, T. & Yamamoto, N. (1995). *J. Solid State Chem.* **114**, 359–363.
Oka, Y., Tamada, O., Yao, T. & Yamamoto, N. (1996). *J. Solid State. Chem.* **126**, 65–73.
Oka, Y., Yao, T. & Yamamoto, N. (1990). *J. Solid State Chem.* **89**, 372–377.
Oka, Y., Yao, T. & Yamamoto, N. (1995*a*). *J. Mater. Chem.* **5**, 1423–1426.
Oka, Y., Yao, T. & Yamamoto, N. (1995*b*). *J. Solid State Chem.* **117**, 407–411.
Oka, Y., Yao, T. & Yamamoto, N. (1997). *J. Solid State Chem.* **132**, 323–329.
Oka, Y., Yao, T., Yamamoto, N. & Ueda, Y. (1998). *J. Solid State Chem.* **141**, 133–139.
Oka, Y., Yao, T., Yamamoto, N., Ueda, Y. & Hayashi, A. (1993). *J. Solid State Chem.* **105**, 271–278.
Ozerov, R. P., Gol'der, G. A. & Zhdanov, G. S. (1957). *Kristallografiya*, **2**, 217–224.
Pecquenard, B., Castro-Garcia, S., Livage, J., Zavalij, P. Y., Whittingham, M. S. & Thouvenot, R. (1998). *Chem. Mater.* **10**, 1882–1888.
Pecquenard, B., Zavalij, P. Y. & Whittingham, M. S. (1998). *Acta Cryst.* C**54**, 1833–1835.
Picciotto, L. A. de, Adendorff, K. T., Liles, D. C. & Thackeray, M. M. (1993). *Solid State Ion.* **62**, 297–307.
Post, J. E. & Bish, D. L. (1988). *Am. Mineral.* **73**, 861–869.
Range, K. J., Eglmeier, C., Heyns, A. M. & de Waal, D. (1990). *Z. Naturforsch.* **45**, 31–38.
Range, K. J. & Zintl, R. (1983). *Mater. Res. Bull.* **18**, 411–419.
Range, K. J. & Zintl, R. (1988). *Z. Naturforsch. Teil B*, **43**, 309–317.
Riou, D. & Férey, G. (1995). *J. Solid State. Chem.* **120**, 137.
Riou, D. & Férey, G. (1996). *Inorg. Chem.* **34**, 6520–6523.
Riou, D., Roubeau, O. & Férey, G. (1998). *Z. Anorg. Allg. Chem.* **624**, 1021–1025.
Rogers, K. D. (1993). *Powder Diffr.* pp. 240–244.
Rozier, P., Savariault, J.-M. & Galy, J. (1996). *J. Solid State Chem.* **122**, 303–308.
Rziha, T., Gies, H. & Rius, J. (1996). *Eur. J. Miner.* **8**, 675–686.
Saux, M. & Galy, J. (1973). *C. R. Acad. Sci. Ser. C*, **276**, 81–84.
Savariault, J.-M., Parize, J.-L., Ballivet-Tkatchenko, D. & Galy, J. (1996). *J. Solid State Chem.* **122**, 1–6.
Schnuriger, B., Enjalbert, R., Savariault, J. M. & Galy, J. (1991). *J. Solid State Chem.* **95**, 397–402.
Shao, M., Leng, J., Pan, Z., Zeng, H. & Tang, Y. (1990). *Gaodeng Xuexiao Huaxue Xuebao*, **11**, 280–285.
Shiro, M. & Fernando, Q. (1971). *Anal. Chem.* **43**, 1222–1230.
Shriver, D. F., Atkins, P. & Langford, C. H. (1994). *Inorganic Chemistry*, 2nd ed., pp. 331–333. New York, USA: W. H. Freeman and Company.
Shustrovitch, E. M., Pori-Koshits, M. A. & Buslaev, Yu. A. (1975). *Coord. Chem. Rev.* **17**, 1–12.
Sokolova, E. V., Simonov, M. A., Karyakin, Yu. V. & Zaval'skaya, A. V. (1983). *Kristallografiya*, **28**, 862–865.
Tamada, O. & Yamamoto, N. (1986). *Miner. J. Jpn*, **13**, 130–140.
Turner, S. & Post, J. E. (1988). *Am. Mineral.* **73**, 1155–1161.
Ueda, Y. (1998). *Chem. Mater.* **10**, 2653–2664.
Vejux, A. & Courtine, P. (1986). *J. Solid State Chem.* **63**, 179–190.
Wadsley, A. D. (1955). *Acta Cryst.* **8**, 695–701.
Walk, C. R. & Gore, J. S. (1975). *J. Electrochem. Soc.* **122**, 68C–68C.
Waltersson, K. & Forslund, B. (1977*a*). *Acta Cryst.* B**33**, 780–784.
Waltersson, K. & Forslund, B. (1977*b*). *Acta Cryst.* B**33**, 784–789.
Waltersson, K. & Forslund, B. (1977*c*). *Acta Cryst.* B**33**, 789–793.
Waltersson, K., Forslund, B., Wilhelmi, K. A., Andersson, S. & Galy, J. (1974). *Acta Cryst.* B**30**, 2644–2652.
Wang, X., Liu, L., Bontchev, R. & Jacobson, A. J. (1998). *Chem. Commun.* pp. 1009–1010.
Weeks, C., Zavalij, P. Y. & Whittingham, M. S. (1999). *Inorg. Chem.* In the press.
Wells, A. F. (1986). *Structural Inorganic Chemistry*, 5th ed. Oxford University Press.
Whittingham, M. S. (1976). *J. Electrochem. Soc.* **123**, 315–320.
Whittingham, M. S., Chen, R., Chirayil, T. & Zavalij, P. Y. (1996). *Electrochem. Soc. Proc.* **96-5**, 76–85.
Wilhelmi, K. A. & Waltersson, K. (1970). *Acta Chem. Scand.* **24**, 3409–3411.
Wilhelmi, K. A., Waltersson, K. & Kihlborg, L. (1971). *Acta Chem. Scand.* **25**, 2675–2687.
Yamase, T. & Ohtaka, K. (1994). *J. Chem. Soc. Dalton Trans.* pp. 2599–2608.
Yao, T., Oka, Y. & Yamamoto, N. (1994). *J. Solid State Chem.* **112**, 196–198.
Zandbergen, H. W., Crespi, A. M., Skarstad, P. M. & Vente, J. F. (1994). *J. Solid State Chem.* **110**, 167–175.
Zavalij, P. Y., Chirayil, T. & Whittingham, M. S. (1997*a*). *Acta Cryst.* C**53**, 879–881.
Zavalij, P. Y., Chirayil, T. & Whittingham, M. S. (1997*b*). *Z. Kristallogr.* **212**, 321–322.
Zavalij, P. Y., Whittingham, M. S., Boylan, E. A., Pecharsky, V. K. & Jacobson, R. A. (1996). *Z. Kristallogr.* **211**, 464–464.
Zavalij, P. Y., Whittingham, M. S., Chirayil, T., Pecharsky, V. K. & Jacobson, R. A. (1997). *Acta Cryst.* C**53**, 170–171.
Zavalij, P. Y., Zhang, F. & Whittingham, M. S. (1999). *Acta Cryst.* Accepted for publication.
Zhang, Y., DeBord, J. R. D., O'Connor, C. J., Haushalter, R. C., Clearfield, A. & Zubieta, J. (1996). *Angew. Chem. Int. Ed. Engl.* **35**, 989–991.
Zhang, Y., Haushalter, R. C. & Clearfield, A. (1996*a*). *Inorg. Chem.* **35**, 4950–4956.
Zhang, Y., Haushalter, R. C. & Clearfield, A. (1996*b*). *Chem. Commun.* pp. 1055–1056.
Zhang, Y., Warren, C. J., Haushalter, R. C., Clearfield, A., Seo, D. K. & Whangbo, M. H. (1998). *Chem. Mater.* **10**, 1059–1064.